TOKAI-HEP/TH-0501

arXiv:hep-ph/0502135v4 17 Apr 2005

Constraints on Flavor Neutrino Masses and $\sin^2 2\vartheta_{12} \gg \sin^2\vartheta_{13}$ in Neutrino Oscillations

Ichiro Aizawa,* Teruyuki Kitabayashi[a†],[‡] and Masaki Yasuè[§]

Department of Physics, Tokai University,
1117 Kitakaname, Hiratsuka,
Kanagawa 259-1291, Japan

[a]*Accelerator Engineering Center*
Mitsubishi Electric System & Service Engineering Co.Ltd.
2-8-8 Umezono, Tsukuba, Ibaraki 305-0045, Japan

(Dated: February, 2005)

To realize the condition of $\sin^2 2\vartheta_{12} \gg \sin^2\vartheta_{13}$, we find constraints on flavor neutrino masses M_{ij} ($ij = e, \mu, \tau$): C1) $c^2_{23}M_{\mu\mu} + s^2_{23}M_{\tau\tau} \approx 2s_{23}c_{23}M_{\mu\tau} + M_{ee}$ and/or C2) $|c_{23}M_{e\mu} - s_{23}M_{e\tau}| \gg |s_{23}M_{e\mu} + c_{23}M_{e\tau}|$, where $c_{23} = \cos\vartheta_{23}$ ($s_{23} = \sin\vartheta_{23}$) and ϑ_{12}, ϑ_{13} and ϑ_{23} are the mixing angles for three flavor neutrinos. The applicability of C1) and C2) is examined in models with one massless neutrino and two massive neutrinos suggested by $\det(M) = 0$, where M is a mass matrix constructed from M_{ij} ($i, j = e, \mu, \tau$). To make definite predictions on neutrino masses and mixings, especially on $\sin\vartheta_{13}$, that enable us to trace C1) and C2), M is assumed to possess texture zeros or to be constrained by textures with $M_{\mu\mu} = M_{\tau\tau}$ or $M_{e\tau} = \pm M_{e\mu}$ which turn out to ensure the emergence of the maximal atmospheric neutrino mixing at $\sin\vartheta_{13} \to 0$. It is found that C1) is used by textures such as $M_{e\mu}$=0 or $M_{e\tau}$=0 while C2) is used by textures such as $M_{e\tau} = \pm M_{e\mu}$.

PACS numbers: 12.60.-i, 13.15.+g, 14.60.Pq, 14.60.St

I. INTRODUCTION

Since the first experimental confirmation of atmospheric neutrino oscillations by Super-Kamiokande [1], there have been various other neutrino oscillations found in solar neutrinos who have given indications for long time [2], accelerator neutrinos and reactor neutrinos [3]. Oscillations of the terrestrial neutrinos turn out to be identical to those of the neutrinos created by the Nature. It is the origin of neutrino oscillations that neutrino have masses [4], which can be created by seesaw mechanism [5, 6] or by radiative mechanism [7, 8]. These neutrino oscillations are explained by the mixings among the known three flavor neutrinos, $\nu_{e,\mu,\tau}$, which are finally converted into three massive neutrinos, $\nu_{1,2,3}$, and are described by their masses of $m_{1,2,3}$ and mixing angles of $\vartheta_{12,23,13}$. The current experimental data of the neutrino oscillations are characterized by the square mass differences for atmospheric neutrinos Δm^2_{atm} with the mixing angle of ϑ_{atm} and for the solar neutrinos $\Delta m^2_\odot$ with the mixing angle of $\vartheta_\odot$. The CHOOZ collaboration has tried to measure another mixing angle ϑ_{CHOOZ}. The result of the observations can be summarized in the following values [9]:

$$\begin{aligned}
&5.4\times10^{-5}eV^2 < \Delta m^2_\odot < 9.5\times10^{-5}eV^2, \quad 0.70 < \sin^2 2\vartheta_\odot < 0.95,\\
&1.2\times10^{-3}eV^2 < \Delta m^2_{atm} < 4.8\times10^{-3}eV^2, \quad 0.92 < \sin^2 2\vartheta_{atm},\\
&\sin\vartheta_{CHOOZ} < 0.23.
\end{aligned} \tag{1}$$

These observed $\Delta m^2_{atm,\odot}$ and the mixing angles can be identified with $\Delta m^2_{atm} = |m^2_3 - m^2_2|$, $\Delta m^2_\odot = |m^2_2 - m^2_1|$, $\vartheta_{atm} = \vartheta_{23}$, $\vartheta_\odot = \vartheta_{12}$ and $\vartheta_{CHOOZ} = \vartheta_{13}$. It should be noted that, from the estimation of effects of matter on solar neutrinos, the mass eigenstate of the larger electron neutrino components ν_1 has the smaller mass than that of the smaller electron neutrino components ν_2 [10]. Thus, the sign of $m^2_2 - m^2_1$ is positive so that $\Delta m^2_\odot = m^2_2 - m^2_1$ (> 0).

One of the remarkable features of the observed neutrino oscillations lies in the fact that $\sin^2 2\vartheta_{12,23} \gg \sin^2\vartheta_{13}$. The almost maximal atmospheric neutrino mixing of $\sin^2 2\vartheta_{23} \sim 1$ may arise as a result of the presence of an approximate

---

[†] Address after April 1, 2005: Department of Physics, Tokai University, 1117 Kitakaname, Hiratsuka, Kanagawa 259-1291, Japan

[*] Electronic address: 4aspd001@keyaki.cc.u-tokai.ac.jp

[‡] Electronic address: teruyuki@keyaki.cc.u-tokai.ac.jp

[§] Electronic address: yasue@keyaki.cc.u-tokai.ac.jp

μ-τ symmetry [11, 12, 13] in flavor neutrino masses forming a symmetric mass matrix of M in the (ν_e, ν_μ, ν_τ)-basis. Namely, the requirement of either $M_{e\mu}=\pm M_{e\tau}$ or $M_{\mu\mu}=M_{\tau\tau}$ ensures the appearance of the maximal atmospheric neutrino mixing at the limit of $\sin\vartheta_{13}\to 0$, where M_{ij} $(i,j=e,\mu,\tau)$ is the flavor neutrino mass for $\nu_i\nu_j$ as an ij-matrix element of M. However, the reason for the large but not maximal mixing of $\sin^2 2\vartheta_{12}$ is not well understood. Some possible answers would be based on the bimaximal mixing scheme [14] relying upon the $L_e-L_\mu-L_\tau$ conservation [15] and on the tri-bimaximal mixing scheme [16, 17, 18], which, respectively, yield $\sin^2 2\vartheta_{12}=1$ with $\sin^2 2\vartheta_{23}$ left undetermined and $\sin^2 2\vartheta_{12}=8/9$ with $\sin^2 2\vartheta_{23}=1$. Before employing such specific schemes, we would like to make more general discussions that guide us to understand the possible form of M to explain the fact of $\sin^2 2\vartheta_{12}\gg\sin^2\vartheta_{13}$.

In this paper, we present expressions to determine ϑ_{12} and ϑ_{13} in terms of M_{ij}, which are given by

$$\tan 2\vartheta_{12}\approx\frac{2\left(c_{23}M_{e\mu}-s_{23}M_{e\tau}\right)}{c_{23}^2M_{\mu\mu}+s_{23}^2M_{\tau\tau}-2s_{23}c_{23}M_{\mu\tau}-M_{ee}},\tag{2}$$

under the approximation of $\sin^2\vartheta_{13}\approx 0$, and

$$\tan 2\vartheta_{13}=\frac{2\left(s_{23}M_{e\mu}+c_{23}M_{e\tau}\right)}{s_{23}^2M_{\mu\mu}+c_{23}^2M_{\tau\tau}+2s_{23}c_{23}M_{\mu\tau}-M_{ee}}.\tag{3}$$

From these expressions, the conditions to have $|\tan 2\vartheta_{12}|\gg|\tan 2\vartheta_{13}|$, namely, $\sin^2 2\vartheta_{12}\gg\sin^2\vartheta_{13}$, can be translated into the conditions among the matrix elements of M. Then, we are able to infer some general underlying properties of M. To have $|\tan 2\vartheta_{12}|\gg|\tan 2\vartheta_{13}|$ can be achieved by the constraints of

- C1) $c_{23}^2M_{\mu\mu}+s_{23}^2M_{\tau\tau}-2s_{23}c_{23}M_{\mu\tau}-M_{ee}\approx 0$ and/or
- C2) $|c_{23}M_{e\mu}-s_{23}M_{e\tau}|\gg|s_{23}M_{e\mu}+c_{23}M_{e\tau}|$.

It should be noted that the sign of s_{23} is crucial for C2) to satisfy $|c_{23}M_{e\mu}-s_{23}M_{e\tau}|\gg|s_{23}M_{e\mu}+c_{23}M_{e\tau}|$ because the cancellation may occur in $s_{23}M_{e\mu}+c_{23}M_{e\tau}$ to reduce its magnitude if the sign of s_{23} is reversed. To see if the requirements from C1) and C2) are plausible, we use explicit models to calculate $\tan 2\vartheta_{13}$ and compare it with $\tan 2\vartheta_{12}$.

Since properties of neutrino oscillations have been clarified in detail by continuous efforts of observing neutrino oscillations [19], the matrix element of M can be completely determined in principle. However, the neutrino mass matrix M at least has 6 parameters and all of these parameters cannot be fixed at present. To somehow determine the texture of M, we need constraints on M, which reduce the number of the independent parameters in M, so that the texture can be determined by the observed data. For example, such constraints are supplied by the condition that the texture includes some zeros in matrix elements of M [20, 21] and by the flavor-basis independent conditions on M such as $\det(M)=m_1m_2m_3=0$ [22] and $\mathrm{tr}(M)=m_1+m_2+m_3=0$ [23]. The condition of $\det(M)=0$ is equivalent to at least demand the presence of one massless neutrino. It is further recognized that even if one of the neutrino mass eigenstates, m_1 or m_3, is exactly zero, we can still explain the observed neutrino oscillation data [22]. This fact suggests that the condition of $\det(M)=0$ is not merely an artificial assumption to reduce the number of independent parameters but can be regarded as a physical assumption that requires the presence of one massless neutrino (or one extremely light neutrino) in the Nature. In fact, the extremely light neutrino of $m_1\sim 10^{-10}$ eV may account [24] for the Affleck-Dine scenario [25] for leptogenesis [26].

We would like to examine possible textures consistent with the observed neutrino properties and to predict allowed regions of the phenomenologically viable angle of ϑ_{13} [27, 28] to be compared with $\sin^2 2\vartheta_{12}$. To see the applicability of C1) and C2) in various textures, we directly compute flavor neutrino masses, where we can trace the source generating $|\tan 2\vartheta_{12}|\gg|\tan 2\vartheta_{13}|$ to see how C1) and C2) work. We focus on models, where one massless neutrino with either $m_1=0$ or $m_3=0$ is present, and examine textures with one vanishing matrix element and with some relations between matrix elements that ensure the appearance of the maximal atmospheric neutrino mixing in the limit of $\sin\theta_{13}\to 0$. The latter textures are suggested by the μ-τ symmetry [11, 12, 13]. From Eq.(3), we will find that the suppressed magnitude of $\sin\vartheta_{13}$ of $\mathcal{O}(0.1)$ reflects that of $M_{e\mu,e\tau}$ and that to obtain more suppressed magnitude of $\sin\vartheta_{13}$ of $\mathcal{O}(0.01)$ needs the cancellation due to $s_{23}M_{e\mu}+c_{23}M_{e\tau}\sim 0$. For instance, it will be shown that the texture with $M_{e\mu}=0$ (or $M_{e\tau}=0$), which cannot have $s_{23}M_{e\mu}+c_{23}M_{e\tau}\sim 0$, turns out to "naturally" predict the larger magnitude of $\sin\vartheta_{13}\gtrsim 0.1$ in the so-called normal mass hierarchy (NMH) with $|m_1|(=0)\ll|m_2|\ll|m_3|$ while, in the so-called inverted mass hierarchy (IMH) with $|m_1|\sim|m_2|\gg|m_3|(=0)$, the observed data is explained by $M_{e\mu}$ or $M_{e\tau}$ itself of $\mathcal{O}(0.01)$ in the same textures, which is "unnaturally" suppressed.

In the next section, we discuss general theoretical consequences of the form of M constrained from the experimental data, which include the useful expression of $\tan 2\vartheta_{12,13}$. In Sec.III, we examine each texture to calculate masses and mixing angles, especially to clarify how to yield the suppressed $\sin^2\theta_{13}$ and to find the possible origin for $\sin^2 2\vartheta_{12}\gg\sin\vartheta_{13}$ in various allowed textures. The final section is devoted to summary and discussions.

II. GENERAL CONSTRAINTS ON FLAVOR NEUTRINO MASSES

Before going into discussions of specific models, where one massless neutrino is present, we use general formulas to add constraints on the masses and mixing angles in terms of the flavor neutrino masses. Our flavor neutrino mass matrix, M, is defined by[1]

$$M = \begin{pmatrix} M_{ee} & M_{e\mu} & M_{e\tau} \\ M_{e\mu} & M_{\mu\mu} & M_{\mu\tau} \\ M_{e\tau} & M_{\mu\tau} & M_{\tau\tau} \end{pmatrix}. \tag{4}$$

The flavor neutrinos $|\nu_{\ell=e,\mu,\tau}\rangle$ and their mass eigenstates $|\nu_{i=1,2,3}\rangle$ are known to be related by $|\nu_\ell\rangle = U_{\ell i}|\nu_i\rangle$ to yield $U^T M U$=diag.(m_1, m_2, m_3) [4], where U represents the unitary transformation usually parameterized by

$$U = \begin{pmatrix} c_{12}c_{13} & s_{12}c_{13} & s_{13} \\ -s_{12}c_{23} - c_{12}s_{23}s_{13} & c_{12}c_{23} - s_{12}s_{23}s_{13} & s_{23}c_{13} \\ s_{12}s_{23} - c_{12}c_{23}s_{13} & -c_{12}s_{23} - s_{12}c_{23}s_{13} & c_{23}c_{13} \end{pmatrix}, \tag{5}$$

where $c_{ij} \equiv \cos\vartheta_{ij}$ and $s_{ij} \equiv \sin\vartheta_{ij}$, and we assume no CP violation in the lepton sector.[2]

From the results in the Appendix A, we can derive the following important properties of M. In the ideal case with $\sin\vartheta_{13}$=0, Eq.(A6) demands that $s_{23}M_{e\mu} + c_{23}M_{e\tau}$=0, from which the maximal atmospheric mixing with $c_{23} = \sigma s_{23} = 1/\sqrt{2}$ for $\sigma = \pm 1$ can be derived by requiring that $M_{e\tau} = -\sigma M_{e\mu}$. Furthermore, Eq.(A7) with the maximal atmospheric mixing reads $M_{\tau\tau} = M_{\mu\mu} + 2s_{13}X$ (unless $M_{\mu\tau} = 0$), from which the requirement of $M_{\tau\tau} = M_{\mu\mu}$ yields either $X(= c_{23}M_{e\mu} - s_{23}M_{e\tau}) = 0$ leading to $M_{e\mu} = \sigma M_{e\tau}$ or $\sin\vartheta_{13}$=0.[3] Therefore, we observe that the almost maximal atmospheric mixing can arise if

$$M_{e\tau} \approx -\sigma M_{e\mu} \text{ and/or } M_{\tau\tau} \approx M_{\mu\mu}, \tag{6}$$

as $\sin\vartheta_{13} \to 0$ and if

$$M_{e\tau} \approx \sigma M_{e\mu} \text{ and } M_{\tau\tau} \approx M_{\mu\mu}, \tag{7}$$

irrespective of the magnitude of $\sin\vartheta_{13}$. Because $X \approx 0$ in Eq.(7), giving $m_1 \approx m_2$ from Eq.(A9), the condition of Eq.(7) is only possible to be satisfied in IMH with $|m_1| \sim |m_2| \gg |m_3|$. If $M_{\tau\tau} \approx M_{\mu\mu}$ and $|M_{e\mu}| \approx |M_{e\tau}|$ are simultaneously satisfied, these relations imply the presence of the (approximate) μ-τ permutation symmetry for the neutrino masses [11, 12, 13]. This realization of $\sin^2 2\vartheta_{23} \sim 1$ and $\sin\vartheta_{13} \sim 0$ is in a sense "natural" because it arises from the consequence of the symmetry principle. However, it may be a real physics that accidentally yields $M_{\mu\mu} \sim M_{\tau\tau}$ for $\sin^2 2\vartheta_{23} \sim 1$ with a suppressed magnitude of $\sin\vartheta_{13}$, which demands the suppression of $M_{e\mu,e\tau}$ itself:

$$|s_{23}^2 M_{\mu\mu} + c_{23}^2 M_{\tau\tau} + 2s_{23}c_{23}M_{\mu\tau} - M_{ee}| \gg |M_{e\mu}|, |M_{e\tau}|, \tag{8}$$

in $\tan 2\vartheta_{13}$ of Eq.(A6). A typical example to be found is a texture with $M_{e\mu} = 0$ or $M_{e\tau} = 0$ for IMH.

In NMH, since $\Delta m^2_{atm} \gg \Delta m^2_\odot$, we find that $|m_{1,2}| \ll |m_3|$, which becomes $|\lambda_{1,2}| \ll |\lambda_3|$ because of Eq.(A10) and $m_3 \sim \lambda_3$ for $\sin^2\vartheta_{13} \ll 1$. The requirement of $|\lambda_2| \ll |\lambda_3|$ gives $|c_{23}^2 M_{\mu\mu} + s_{23}^2 M_{\tau\tau} - 2s_{23}c_{23}M_{\mu\tau}| \ll |s_{23}^2 M_{\mu\mu} + c_{23}^2 M_{\tau\tau} + 2s_{23}c_{23}M_{\mu\tau}|$, which roughly yields,

$$c_{23}^2 M_{\mu\mu} + s_{23}^2 M_{\tau\tau} \sim 2s_{23}c_{23}M_{\mu\tau}, \tag{9}$$

leading to

$$M_{\mu\mu} + M_{\tau\tau} \sim 2\sigma M_{\mu\tau}, \tag{10}$$

---

[1] It is understood that the charged leptons and neutrinos are rotated, if necessary, to give diagonal charged-current interactions and to define ν_e, ν_μ and ν_τ.

[2] For M allowing CP-violation, see discussions in Ref.[29].

[3] For the texture with $M_{\mu\mu \text{ or } \tau\tau} = 0$, the maximal atmospheric neutrino mixing cannot be realized as a result of $\cos 2\vartheta_{23} = 0$, which does not satisfy Eq.(A7). Instead, $\sigma M_{e\mu} + M_{e\tau} \sim 0$ is to be satisfied. It is understood that this texture is excluded for $M_{\mu\mu} \sim M_{\tau\tau}$.

for $c_{23} \sim \sigma s_{23} \sim 1/\sqrt{2}$. It is satisfied by textures of NMH to be discussed in Sec.III. Since $M_{\mu\mu} \sim M_{\tau\tau}$ from Eq.(A7) for $c_{12} \sim \sigma s_{23} \sim 1/\sqrt{2}$ (except for $M_{\mu\mu \text{ or } \tau\tau} = 0$), it implies a more constrained relation of $M_{\mu\mu} \sim M_{\tau\tau} \sim \sigma M_{\mu\tau}$ or even the ideal situation of

$$M_{\mu\mu} = M_{\tau\tau} = \sigma M_{\mu\tau}, \tag{11}$$

that suggests the presence of democratic interactions among $\nu_{\mu,\tau}$ in neutrino physics.

Similarly, in IMH, from $\Delta m^2_{atm} \gg \Delta m^2_{\odot}$, we find that $|m_1| \sim |m_2| \gg |m_3|$ requiring $m_1 \sim \pm m_2$, which becomes $|\lambda_{1,2}| \gg |\lambda_3|$. The requirement of $|\lambda_{1,2}| \gg |\lambda_3|$ instead gives $\lambda_3 \sim 0$

$$s^2_{23} M_{\mu\mu} + c^2_{23} M_{\tau\tau} \sim -2 s_{23} c_{23} M_{\mu\tau}, \tag{12}$$

leading to

$$M_{\mu\mu} + M_{\tau\tau} \sim -2\sigma M_{\mu\tau}. \tag{13}$$

The textures with IMH are to be found to generally exhibit Eq.(13). Again, the situation of

$$M_{\mu\mu} = M_{\tau\tau} = -\sigma M_{\mu\tau} \tag{14}$$

may be realized in "ideal" neutrino physics. Furthermore, Eq.(A10) leads to $\lambda_1 \sim \lambda_2$ for $m_1 \sim m_2$ provided that $|\lambda_1 + \lambda_2| \gg |X|$ and to $\lambda_1 \sim -\lambda_2$ for $m_1 \sim -m_2$ provided that $|\lambda_1 + \lambda_2| \ll |X|$. In terms of M_{ij}, these constraints can be expressed as

$$c^2_{23} M_{\mu\mu} + s^2_{23} M_{\tau\tau} - 2 s_{23} c_{23} M_{\mu\tau} \sim \pm M_{ee}, \tag{15}$$

for $m_1 \sim \pm m_2$. For $c_{23} \sim \sigma s_{23} \sim 1/\sqrt{2}$, it leads to

$$M_{\mu\mu} + M_{\tau\tau} - 2\sigma M_{\mu\tau} \sim \pm 2 M_{ee}. \tag{16}$$

An additional constraint on $\lambda_{1,2}$ arises in the case of $|X| \ll |\lambda_1 + \lambda_2|$ ($m_1 \sim m_2$) suggesting $X \sim 0$. We will find that, in the textures such as those with $M_{e\mu} = 0$ and $M_{e\tau} = 0$ giving X=$c_{23} M_{e\mu}/c_{13}$ and $-s_{23} M_{e\tau}/c_{13}$, the large suppression of X directly requires the large suppression of $M_{e\mu}$ or $M_{e\tau}$ itself, which is the similar to Eq.(8). While if $M_{e\mu}/M_{e\tau} \sim \tan\vartheta_{23}$ can be satisfied, the large suppression is not required to give $X \sim 0$ such as in the textures with $M_{e\tau} = \pm M_{e\mu}$.

Once these results are obtained, it is useful to express the flavor neutrino masses as follows:

$$\begin{aligned}
M_{ee} &= c^2_{13}\left(c^2_{12} m_1 + s^2_{12} m_2\right) + s^2_{13} m_3, \\
M_{e\mu} &= s_{23} s_{13} c_{13}\left[m_3 - \left(c^2_{12} m_1 + s^2_{12} m_2\right)\right] - s_{12} c_{12} c_{23} c_{13}\left(m_1 - m_2\right), \\
M_{e\tau} &= c_{23} s_{13} c_{13}\left[m_3 - \left(c^2_{12} m_1 + s^2_{12} m_2\right)\right] + s_{12} c_{12} s_{23} c_{13}\left(m_1 - m_2\right), \\
M_{\mu\mu} &= c^2_{23}\left(s^2_{12} m_1 + c^2_{12} m_2\right) + s^2_{23} s^2_{13}\left(c^2_{12} m_1 + s^2_{12} m_2\right) + s^2_{23} c^2_{13} m_3 + 2 s_{12} c_{12} s_{23} c_{23} s_{13}\left(m_1 - m_2\right), \\
M_{\mu\tau} &= s_{23} c_{23}\left[s^2_{13}\left(c^2_{12} m_1 + s^2_{12} m_2\right) - \left(s^2_{12} m_1 + c^2_{12} m_2\right) + c^2_{13} m_3\right] + s_{12} c_{12}\left(c^2_{23} - s^2_{23}\right) s_{13}\left(m_1 - m_2\right), \\
M_{\tau\tau} &= s^2_{23}\left(s^2_{12} m_1 + c^2_{12} m_2\right) + c^2_{23} s^2_{13}\left(c^2_{12} m_1 + s^2_{12} m_2\right) + c^2_{23} c^2_{13} m_3 - 2 s_{12} c_{12} s_{23} c_{23} s_{13}\left(m_1 - m_2\right).
\end{aligned} \tag{17}$$

Using $c_{23} \sim \sigma s_{23} \sim 1/\sqrt{2}$ and $s_{13} \sim 0$ as well as $|m_1| < |m_2| \ll |m_3|$ in NMH and $|m_2| > |m_1| \gg |m_3|$ in IMH, we can readily understand that why the obtained constraints are so satisfied.

In addition to these constraints, from Eq.(A6), we notice another constraint derived from the similarity between the expressions of $\tan 2\vartheta_{12}$ and $\tan 2\vartheta_{13}$, which are given by Eq.(2) because of $\lambda_1 \sim M_{ee}$ for $\sin^2\vartheta_{13} \sim 0$ and Eq.(3), which turn out to be more symmetric expressions:

$$\tan 2\vartheta_{12} \sim \frac{2\sqrt{2}\left(M_{e\mu} - \sigma M_{e\tau}\right)}{M_{\mu\mu} + M_{\tau\tau} - 2\sigma M_{\mu\tau} - 2M_{ee}}, \tag{18}$$

$$\tan 2\vartheta_{13} \sim \frac{2\sqrt{2}\left(\sigma M_{e\mu} + M_{e\tau}\right)}{M_{\mu\mu} + M_{\tau\tau} + 2\sigma M_{\mu\tau} - 2M_{ee}}, \tag{19}$$

under the approximation of $c_{23} \sim \sigma s_{23} \sim 1/\sqrt{2}$. This similarity is useful to see how $\sin^2 2\vartheta_{12} \gg \sin^2\vartheta_{13}$ is realized. As stated in the Introduction, the relation of $\sin^2 2\vartheta_{12} \gg \sin^2\vartheta_{13}$ is typically expected to arise from the constraints of C1) and C2), where $s_{23} M_{e\mu} + c_{23} M_{e\tau} \sim 0$ is probable for the latter case. In IMH, combined with Eq.(15), these conditions lead to C1) for $m_1 \sim m_2$ and C2) with $s_{23}^2 M_{\mu\mu} + c_{23}^2 M_{\tau\tau} \approx 2 s_{23} c_{23} M_{\mu\tau} - M_{ee}$ for $m_1 \sim -m_2$. If C1) is realized, we obtain that $\lambda_3 \sim M_{\mu\mu} + M_{\tau\tau} - M_{ee}$ and

$$\tan 2\vartheta_{13} \approx \frac{2\left(s_{23} M_{e\mu} + c_{23} M_{e\tau}\right)}{M_{\mu\mu} + M_{\tau\tau} - 2M_{ee}}. \tag{20}$$

In IMH, since $\lambda_1 \sim M_{ee}$ for $\sin^2\vartheta_{13} \sim 0$, $\lambda_3 \sim m_3$ and $(|m_3| \ll)|m_{1,2}| \sim |\lambda_{1,2}|$ from Eq.(A10), we obtain $|\lambda_3| \ll |M_{ee}|$, which directly gives

$$\tan 2\vartheta_{13} \approx -\frac{2\left(s_{23} M_{e\mu} + c_{23} M_{e\tau}\right)}{M_{ee}}, \tag{21}$$

from $\tan 2\vartheta_{13}$ of Eq.(A6).

We have sufficient conditions that can be reshuffled to give other useful constraints. In the case of $M_{\mu\mu} \sim M_{\tau\tau}$ for the almost maximal atmospheric neutrino mixing, two conditions of $M_{\mu\mu} + M_{\tau\tau} \sim 2\sigma M_{\mu\tau} + 2M_{ee}$ for $\sin^2 2\vartheta_{12} \gg \sin^2\vartheta_{13}$ as C1) and $M_{\mu\mu} + M_{\tau\tau} \sim 2\sigma M_{\mu\tau}$ for $|\Delta m^2_{atm}| \gg \Delta m^2_\odot$ yield

$$|M_{\mu\mu} + M_{\tau\tau}| \gg |M_{ee}|, \tag{22}$$

in NMH. On the other hand, in IMH, those of $M_{\mu\mu} + M_{\tau\tau} \sim 2\sigma M_{\mu\tau} \pm 2M_{ee}$ for $m_1 \sim \pm m_2$ and $M_{\mu\mu} + M_{\tau\tau} \sim -2\sigma M_{\mu\tau}$ for $|\Delta m^2_{atm}| \gg \Delta m^2_\odot$ yield

$$M_{\mu\mu} + M_{\tau\tau} \sim \pm M_{ee}, \quad 2\sigma M_{\mu\tau} \sim \mp M_{ee}. \tag{23}$$

The texture with $M_{ee} = 0$ in IMH does not explain $|m_1| \sim |m_2|$. For $m_1 \sim m_2$, owing to the constraint of $M_{\mu\mu} + M_{\tau\tau} \sim M_{ee}$, Eqs.(20) and (21) applied to IMH become consistent with each other. These results are summarized in TABLE I.

To see how $\sin^2 2\vartheta_{12} \gg \sin^2\vartheta_{13}$ is numerically obtained, we use the "theoretical" data to be collected in the next section, where we assume the interesting possibility that the Nature enjoys the presence of one massless neutrino. For the rest of discussions, we employ models with texture zeros and with $M_{\mu\mu}$=$M_{\tau\tau}$ and $M_{e\tau} = \pm M_{e\mu}$ and find allowed regions for $\sin\vartheta_{13}$ in each texture.

III. SPECIFIC TEXTURES

Now, the determinant zero condition is used to ensure the presence of one massless neutrino, which allows the only two cases to be compatible with the observation: (m_1, m_2, m_3)=$(0, \pm\sqrt{\Delta m^2_\odot}, \pm\sqrt{\Delta m^2_{atm} + \Delta m^2_\odot})$ leading to $|m_3| \gg |m_2|$ and $(m_1, m_2, m_3) = (\pm\sqrt{\Delta m^2_{atm}}, \pm\sqrt{\Delta m^2_{atm} + \Delta m^2_\odot}, 0)$ leading to $|m_1| \sim |m_2|$. The case with $(0, m_2, m_3)$ corresponds NMH while the case with $(m_1, m_2, 0)$ corresponds to IMH. In NMH, we find that

$$\tan^2\vartheta_{12} = \frac{\lambda_1}{\lambda_2}, \tag{24}$$

to realize $m_1 = 0$ in Eq.(A10).

By requiring in Eq.(17) that one of the matrix elements vanishes or that the relations of $M_{\mu\mu} = M_{\tau\tau}$ and $M_{e\tau} = \pm M_{e\mu}$ are satisfied, we obtain the following constraints for the ratio of m_3/m_2 in NMH with $m_1 = 0$:

$$\begin{aligned}
&M_{ee} = 0 \;\rightarrow\; \frac{m_3}{m_2} = -\frac{s_{12}^2 c_{13}^2}{s_{13}^2}, \qquad M_{e\mu} = 0 \rightarrow \frac{m_3}{m_2} = -\frac{s_{12}c_{12}c_{23} - s_{12}^2 s_{23} s_{13}}{s_{23} s_{13}},\\
&M_{e\tau} = 0 \;\rightarrow\; \frac{m_3}{m_2} = \frac{s_{12}c_{12}s_{23} + s_{12}^2 c_{23} s_{13}}{c_{23} s_{13}}, \quad M_{\mu\mu} = 0 \rightarrow \frac{m_3}{m_2} = -\frac{c_{12}^2 c_{23}^2 + s_{12}^2 s_{23}^2 s_{13}^2 - 2 s_{12}c_{12}s_{23}c_{23}s_{13}}{s_{23}^2 c_{13}^2},\\
&M_{\mu\tau} = 0 \;\rightarrow\; \frac{m_3}{m_2} = \frac{\left(c_{12}^2 - s_{12}^2 s_{13}^2\right) s_{23}c_{23} + s_{12}c_{12}\left(c_{23}^2 - s_{23}^2\right) s_{13}}{s_{23}c_{23}c_{13}^2},\\
&M_{\tau\tau} = 0 \;\rightarrow\; \frac{m_3}{m_2} = -\frac{c_{12}^2 s_{23}^2 + s_{12}^2 c_{23}^2 s_{13}^2 + 2 s_{12}c_{12}s_{23}c_{23}s_{13}}{c_{23}^2 c_{13}^2},\\
&M_{\mu\mu} = M_{\tau\tau} \;\rightarrow\; \frac{m_3}{m_2} = \frac{(c_{12}^2 - s_{12}^2 s_{13}^2)(c_{23}^2 - s_{23}^2) - 4 s_{12}c_{12}s_{23}c_{23}s_{13}}{(c_{23}^2 - s_{23}^2) c_{13}^2},\\
&M_{e\tau} = \eta M_{e\mu} \;\rightarrow\; \frac{m_3}{m_2} = \frac{s_{12}^2\left(c_{23} - \eta s_{23}\right) s_{13} + s_{12}c_{12}\left(\eta c_{23} + s_{23}\right)}{(c_{23} - \eta s_{23}) s_{13}},
\end{aligned} \tag{25}$$

where $\eta = \pm 1$. We can also obtain the following constraints for the ratio of m_2/m_1 in IMH with $m_3 = 0$:

$$\begin{aligned}
M_{ee} = 0 &\rightarrow \frac{m_2}{m_1} = -\frac{c^2_{12}}{s^2_{12}}, \qquad M_{e\mu} = 0 \rightarrow \frac{m_2}{m_1} = \frac{s_{12}c_{12}c_{23} + c^2_{12}s_{23}s_{13}}{s_{12}c_{12}c_{23} - s^2_{12}s_{23}s_{13}},\\
M_{e\tau} = 0 &\rightarrow \frac{m_2}{m_1} = \frac{s_{12}c_{12}s_{23} - c^2_{12}c_{23}s_{13}}{s_{12}c_{12}s_{23} + s^2_{12}c_{23}s_{13}}, \quad M_{\mu\mu} = 0 \rightarrow \frac{m_2}{m_1} = -\frac{s^2_{12}c^2_{23} + c^2_{12}s^2_{23}s^2_{13} + 2s_{12}c_{12}s_{23}c_{23}s_{13}}{c^2_{12}c^2_{23} + s^2_{12}s^2_{23}s^2_{13} - 2s_{12}c_{12}s_{23}c_{23}s_{13}},\\
M_{\mu\tau} = 0 &\rightarrow \frac{m_2}{m_1} = -\frac{\left(s^2_{12} - c^2_{12}s^2_{13}\right)s_{23}c_{23} - s_{12}c_{12}\left(c^2_{23} - s^2_{23}\right)s_{13}}{\left(c^2_{12} - s^2_{12}s^2_{13}\right)s_{23}c_{23} + s_{12}c_{12}\left(c^2_{23} - s^2_{23}\right)s_{13}},\\
M_{\tau\tau} = 0 &\rightarrow \frac{m_2}{m_1} = -\frac{s^2_{12}s^2_{23} + c^2_{12}c^2_{23}s^2_{13} - 2s_{12}c_{12}s_{23}c_{23}s_{13}}{c^2_{12}s^2_{23} + s^2_{12}c^2_{23}s^2_{13} + 2s_{12}c_{12}s_{23}c_{23}s_{13}},\\
M_{\mu\mu} = M_{\tau\tau} &\rightarrow \frac{m_2}{m_1} = -\frac{\left(s^2_{12} - c^2_{12}s^2_{13}\right)\left(c^2_{23} - s^2_{23}\right) + 4s_{12}c_{12}s_{23}c_{23}s_{13}}{\left(c^2_{12} - s^2_{12}s^2_{13}\right)\left(c^2_{23} - s^2_{23}\right) - 4s_{12}c_{12}s_{23}c_{23}s_{13}},\\
M_{e\tau} = \eta M_{e\mu} &\rightarrow \frac{m_2}{m_1} = -\frac{c^2_{12}\left(c_{23} - \eta s_{23}\right)s_{13} - s_{12}c_{12}\left(\eta c_{23} + s_{23}\right)}{s^2_{12}\left(c_{23} - \eta s_{23}\right)s_{13} + s_{12}c_{12}\left(\eta c_{23} + s_{23}\right)}. \qquad (26)
\end{aligned}$$

Using the experimental data of $\Delta m^2_{atm,\odot}$, we find the upper and lower limits of m^2_3/m^2_2 for NMH and of m^2_2/m^2_1 for IMH as shown in Table II. These ratios are calculated from Eqs.(25) and (26) with the observed mixing angles in Eq.(1). As already pointed out in the Introduction, the sign of s_{23} is considered to obtain s_{13} because s_{13} is proportional to $Y = s_{23}M_{e\mu} + c_{23}M_{e\tau}$ as in Eq.(A5),[4] where Y can reduce its magnitude depending upon the sign of s_{23}. From Δm^2_{atm} and $\Delta m^2_{\odot}$, the allowed region of m^2_3/m^2_2 with NMH and of m^2_2/m^2_1 with IMH are computed to be $13.6 \leq m^2_3/m^2_2 \leq 89.9$ and $1.01 \leq m^2_2/m^2_1 \leq 1.08$, respectively.

We find the allowed textures with

- in the case of NMH,
  - $M_{ee} = 0$, $M_{e\mu} = 0$ and $M_{e\tau} = 0$ as well as $M_{\mu\mu} = M_{\tau\tau}$ and $M_{e\tau} = -M_{e\mu}$ for $\sin\theta_{23} > 0$
  - $M_{ee} = 0$, $M_{e\mu} = 0$ and $M_{e\tau} = 0$ as well as $M_{\mu\mu} = M_{\tau\tau}$ and $M_{e\tau} = M_{e\mu}$ for $\sin\theta_{23} < 0$
- in the case of IMH,
  - $M_{e\mu} = 0$ and $M_{\mu\mu} = 0$ as well as $M_{\mu\mu} = M_{\tau\tau}$ and $M_{e\tau} = -M_{e\mu}$ for $\sin\theta_{23} > 0$,
  - $M_{e\tau} = 0$ and $M_{\tau\tau} = 0$ as well as $M_{e\tau} = \pm M_{e\mu}$ for $\sin\theta_{23} < 0$,

from Table II. Other textures with one vanishing matrix element are excluded by the observed constraints on the masses and the mixing angles. In NMH, the allowed textures have the property that m_3/m_2 gets increased either as $c^2_{23} \rightarrow s^2_{23}$ ($\sin^2 2\theta_{23} \rightarrow 1$) for $M_{\mu\mu} = M_{\tau\tau}$ or as $s_{13} \rightarrow 0$ for other textures to meet the experimentally allowed value of m^2_3/m^2_2. It is thus expected that $\sin^2 2\theta_{23} \approx 1.0$ in the texture with $M_{\mu\mu} = M_{\tau\tau}$. The texture with two zeros such as $M_{e\mu}$=$M_{e\tau}$=0 is excluded simply because $\tan^2\vartheta_{23} = -1$ is satisfied. Similarly for other excluded textures.

Shown in TABLE III is the summary of our predictions on the values of $\sin\vartheta_{23}$, which are depicted in FIG.1-FIG.13. The effective neutrino mass $m_{\beta\beta}$ used in the detection of the absolute neutrino mass [30] is computed in each texture and the lower and upper bounds on $m_{\beta\beta}$ ($=M_{ee}$) in the present discussions are tabulated in TABLE IV. Also computed in TABLE V and TABLE VI is each element of M for the typical values of mixing angles such as $\sin^2 2\vartheta_{12} = 0.80$ and $\sin^2 2\vartheta_{12} = 0.98$ to see how $\sin^2\theta_{13} \ll 1$ as well as some hierarchies among $\lambda_{1,2,3}$ are realized. The following characteristic features of the textures are found from these tables and figures:

1. The announced relations of $M_{\mu\mu} + M_{\tau\tau} \sim 2\sigma M_{\mu\tau}$ and $|M_{\mu\mu} + M_{\tau\tau}| \gg |M_{ee}|$ in NMH and of $M_{\mu\mu} + M_{\tau\tau} \sim -2\sigma M_{\mu\tau}$ and $M_{\mu\mu} + M_{\tau\tau} \sim \pm M_{ee}$ in IMH with $m_1 \sim \pm m_2$ are satisfied.
2. There are additional hierarchies of $|M_{e\mu}|, |M_{e\tau}| \ll |M_{\mu\mu} + M_{\tau\tau}|$ in NMH and of $|M_{ee}| \gg |\sigma M_{e\mu} + M_{e\tau}|$ in IMH. Furthermore, $|M_{e\mu} - \sigma M_{e\tau}| \gg |\sigma M_{e\mu} + M_{e\tau}|$ expected in C2) is satisfied in the IMH-textures with $M_{\mu\mu} = 0$ ($\sigma = 1$), $M_{\tau\tau} = 0$ ($\sigma = -1$), $M_{\mu\mu} = M_{\tau\tau}$ ($\sigma = 1$) and $M_{e\tau} = M_{e\mu}$ ($\sigma = -1$), all exhibiting $m_1 \sim -m_2$.

---

[4] We assume that $s^2_{23} < c^2_{23}$ and do not include the case with $s^2_{23} > c^2_{23}$ because the texture with interchange of $s_{23} \leftrightarrow c_{23}$ accompanied by the appropriate change of the sign of s_{13} becomes identical to one of the existing textures.

3. The suppressed $\tan 2\vartheta_{13}$ is realized by the dominated magnitude of λ_3 ($\sim M_{\mu\mu}+M_{\tau\tau}+2\sigma M_{\mu\tau}$) for NMH and of M_{ee} for IMH (because of $\lambda_3\sim 0$ in Eq.(21)). The more suppressed values of $\sin\vartheta_{13}\lesssim 0.05$ are obtained due to $s_{23}M_{e\mu}+c_{23}M_{e\tau}\sim 0$, which is possible to occur in the textures with $M_{\mu\mu}=M_{\tau\tau}$ (only for IMH) and $M_{e\tau}=\pm M_{e\mu}$.
4. In NMH, $\sin^2 2\vartheta_{23}=0.998$ is selected as a typical value in the texture with $M_{\mu\mu}=M_{\tau\tau}$, which requires that $c^2_{23}\rightarrow s^2_{23}$ in the denominator of m_2/m_1 in Eq.(26) since, in this limit, m_2/m_1 approaches to 1 by passing the experimentally allowed m_2/m_1,
5. In IMH, the small magnitude of $\sin\vartheta_{13}$ calls for the suppressed and almost vanishing $M_{e\mu}$ ($M_{e\tau}$) for the texture with $M_{e\tau}=0$ ($M_{e\mu}=0$).
6. In IMH, the relatively small magnitude of M_{ee} can enhance $\sin\vartheta_{13}$($\gtrsim$0.15) as in Eq.(21) in the textures with $M_{\mu\mu}=0$, $M_{\tau\tau}=0$ and $M_{e\mu}=M_{e\tau}$. The texture with $M_{\mu\mu}=M_{\tau\tau}$ that also shows the relatively small magnitude of M_{ee} receives the cancellation in $s_{23}M_{e\mu}+c_{23}M_{e\tau}(=0.002)$ to yield $\sin\vartheta_{13}=0.037$.
7. In IMH, the source of $m_{1,2}$ comes either from $\lambda_1\sim\lambda_2$ giving $m_2\sim m_1$ for the textures with $M_{e\mu,e\tau}=0$ and $M_{e\tau}=\pm M_{e\mu}$ or from $X/\sin 2\vartheta_{12}$ with $\lambda_1+\lambda_2\sim 0$ giving $m_2\sim -m_1$ for others. Two sources coexist in the texture with $M_{\mu\mu}=M_{\tau\tau}$, where the lower bound on m_2/m_1 arises from the two sources as in FIG.11.
8. In IMH, the upper bounds on m^2_2/m^2_1 in FIG.11 and FIG.13 for $\sin\vartheta_{23}>0$ and in FIG.12 for $\sin\vartheta_{23}<0$ are very steep because, in Eq.(26), either $c^2_{23}-s^2_{23}$ in $M_{\mu\mu}=M_{\tau\tau}$ or $\eta c_{23}+s_{23}$ in $M_{e\tau}=\sigma M_{e\mu}$ can compete with s_{13} so that the cancellation occurs in the denominators around $c^2_{23}\sim s^2_{23}$ ($M_{\mu\mu}=M_{\tau\tau}$) and $\eta c_{23}\sim -s_{23}$ ($M_{e\tau}=\sigma M_{e\mu}$) to give the rapid rise of m^2_2/m^2_1.
9. The effective neutrino mass of $m_{\beta\beta}$ is at most 0.008 eV for NMH and at most 0.07 eV for IMH.

Some of these features are based on the specific values of mixing angles listed in the tables. However, some of the constraints are generally satisfied by Eq.(17) that do not depend on the details of models and it has been checked that these features are shared by other allowed set of values of mixing angles.

Let us finally comment on how to realize $\sin^2 2\vartheta_{12}\gg\sin^2\vartheta_{13}$. In NMH, we have obtained the approximate relations of

$$M_{\mu\mu}+M_{\tau\tau}\sim 2\sigma M_{\mu\tau}, \tag{27}$$

$$|M_{\mu\mu}+M_{\tau\tau}|\gg|M_{ee}|, \tag{28}$$

$$|M_{\mu\mu}+M_{\tau\tau}|\gg|\sigma M_{e\mu}+M_{e\tau}|. \tag{29}$$

Since Eq.(18) leads to

$$\tan 2\vartheta_{12}\sim\frac{2\sqrt{2}\,(M_{e\mu}-\sigma M_{e\tau})}{M_{\mu\mu}+M_{\tau\tau}-2\sigma M_{\mu\tau}}, \tag{30}$$

from Eq.(28) and $|\tan 2\vartheta_{12}|\gg 1$ arises because of Eq.(27); therefore, the constraint of C1) works. We also find from Eq.(28) that Eq.(20) leads to

$$\tan 2\vartheta_{13}\sim\frac{\sqrt{2}\,(\sigma M_{e\mu}+M_{e\tau})}{M_{\mu\mu}+M_{\tau\tau}}, \tag{31}$$

which gives $|\tan\vartheta_{13}|\ll 1$ because of Eq.(29). In IMH, we have obtained the approximate relations of

$$M_{\mu\mu}+M_{\tau\tau}\sim -2\sigma M_{\mu\tau}, \tag{32}$$

$$|\sigma M_{e\mu}+M_{e\tau}|\ll|M_{ee}|, \tag{33}$$

as well as

$$M_{\mu\mu}+M_{\tau\tau}\sim M_{ee}, \tag{34}$$

for $m_1\sim m_2$, and

$$M_{\mu\mu}+M_{\tau\tau}\sim -M_{ee}\sim -2\sigma M_{\mu\tau}, \tag{35}$$

$$|M_{e\mu}-\sigma M_{e\tau}|\gg|\sigma M_{e\mu}+M_{e\tau}|, \tag{36}$$

for $m_1 \sim -m_2$. For $m_1 \sim m_2$,

$$\tan 2\vartheta_{12} \sim \frac{\sqrt{2}\,(M_{e\mu} - \sigma M_{e\tau})}{M_{\mu\mu} + M_{\tau\tau} - M_{ee}}, \tag{37}$$

from Eq.(32), leading to $|\tan 2\vartheta_{12}| \gg 1$ because of Eq.(34). The constraint of C1) works for $m_1 \sim m_2$. From Eq.(21),

$$\tan 2\vartheta_{13} \sim -\frac{\sqrt{2}\,(\sigma M_{e\mu} + M_{e\tau})}{M_{ee}}, \tag{38}$$

is obtained and $|\tan 2\vartheta_{13}| \ll 1$ arises because of Eq.(33) in both $m_1 \sim m_2$ and $m_1 \sim -m_2$. On the other hand, for $m_1 \sim -m_2$, we obtain that

$$\tan 2\vartheta_{12} \sim -\frac{\sqrt{2}\,(M_{e\mu} - \sigma M_{e\tau})}{2M_{ee}}, \tag{39}$$

from Eq.(35). By comparing it with Eq.(38), we observe that $|\tan 2\vartheta_{12}| \gg |\tan 2\vartheta_{13}|$ is due to Eq.(36). The constraint of C2) works for $m_1 \sim -m_2$. Therefore, the constraints of C1) and C2), repectively, work for NMH and IMH with $m_1 \sim m_2$ and for IMH with $m_1 \sim -m_2$ to yield $\sin^2 2\vartheta_{12} \gg \sin^2 \vartheta_{13}$, which also calls for the additional hierarchy of either $|M_{\mu\mu} + M_{\tau\tau}| \gg |s_{12}M_{e\mu} + c_{12}M_{e\tau}|$ (NMH), or $|M_{ee}| \gg |c_{23}M_{e\mu} + s_{23}M_{e\tau}|$ (IMH) to suppress the magnitude of $\sin^2 \vartheta_{13}$ itself. Of course, the cancellation of $c_{23}M_{e\mu} + s_{23}M_{e\tau} \sim 0$ can be one of the sources of this hierarchy.

IV. SUMMARY AND DISCUSSIONS

We have suggested that the almost maximal atmospheric neutrino mixing occurs if

$$M_{e\tau} \approx -\sigma M_{e\mu} \text{ and/or } M_{\tau\tau} \approx M_{\mu\mu}, \tag{40}$$

as $\sin\vartheta_{13} \to 0$ and if

$$M_{e\tau} \approx \sigma M_{e\mu} \text{ and } M_{\tau\tau} \approx M_{\mu\mu}, \tag{41}$$

irrespective of the magnitude of $\sin\vartheta_{13}$. The useful formulas are derived to calculate the mixing angles of $\theta_{12,13}$ in terms of the flavor neutrino masses, M_{ij} for $i, j = e, \mu, \tau$:

$$\tan 2\vartheta_{13} = \frac{2\,(s_{23}M_{e\mu} + c_{23}M_{e\tau})}{s^2_{23}M_{\mu\mu} + c^2_{23}M_{\tau\tau} + 2s_{23}c_{23}M_{\mu\tau} - M_{ee}}, \tag{42}$$

and

$$\tan 2\vartheta_{12} \approx \frac{2\,(s_{23}M_{e\tau} - c_{23}M_{e\mu})}{c^2_{23}M_{\mu\mu} + s^2_{23}M_{\tau\tau} - 2s_{23}c_{23}M_{\mu\tau} - M_{ee}}, \tag{43}$$

as far as $\sin^2\vartheta_{13} \approx 0$. We have suggested the mechanism to obtain the suppressed $\sin\vartheta_{13}$ based on

- the hierarchy of $|M_{ee,\mu\mu,\mu\tau \text{ and/or } \tau\tau}| \gg |\sigma M_{e\mu} + M_{e\tau}|$,
- the cancellation of $s_{23}M_{e\mu} + c_{23}M_{e\tau} \sim 0$ (for more suppressed $\sin\vartheta_{13}$),

and also to yield $\sin^2 2\vartheta_{12} \gg \sin^2\vartheta_{13}$ based on

- the approximate equality of $c^2_{23}M_{\mu\mu} + s^2_{23}M_{\tau\tau} \approx 2s_{23}c_{23}M_{\mu\tau} + M_{ee}$,
- the hierarchy of $|c_{23}M_{e\mu} - s_{23}M_{e\tau}| \gg |s_{23}M_{e\mu} + c_{23}M_{e\tau}|$.

Considering various general constraints on flavor neutrino masses shown in TABLE I, we reach the plausible textures at the "zero"-th order:

$$M^{NMH} = \begin{pmatrix} \epsilon_1 & \epsilon_2 & \epsilon_3 \\ \epsilon_2 & d & \sigma d \\ \epsilon_3 & \sigma d & d \end{pmatrix}, \quad M^{IMH} = \begin{pmatrix} \pm 2d & b & -\sigma b \\ b & d & -\sigma d \\ -\sigma b & -\sigma d & d \end{pmatrix} \text{ (for } m_1 \sim \pm m_2\text{)}, \tag{44}$$

where $|\epsilon_{1,2,3}| \ll |d|$ in M^{NMH} and $\sigma = \pm 1$ for $\sin\vartheta_{23} = \sigma/\sqrt{2}$. It should be noted that the pattern in M^{NMH} may reflect a symmetry based on the approximate conservation of the electron number, L_e. Namely, ϵ_1 has $L_e = 2$, $\epsilon_{2,3}$ have $L_e = 1$ and d has $L_e = 0$ [31, 32]. In the case that the conservation of L_e is perturbatively violated by an interaction of $L_e = \pm 1$ characterized by an appropriate parameter of ξ with $|\xi| \ll 1$ [32], it is not absurd to expect $\epsilon_1 \propto \xi^2$, $\epsilon_{2,3} \propto \xi$ and $d \propto \xi^0$, which explain the required order in M^{NMH}.

In specific models with one massless neutrino, the above-mentioned mechanisms have been confirmed to yield the consistent magnitudes of $\sin\vartheta_{13}$ and $\sin^2 2\vartheta_{12}$ in various textures. The allowed textures are found to exhibit the following patterns of the flavor neutrino masses:

- For NMH, either M_{ee}, $M_{e\mu}$ or $M_{e\tau}$ can vanish and
$$|M_{\mu\mu} + M_{\tau\tau}| \gg |M_{ee}|, |\sigma M_{e\mu} + M_{e\tau}|, \quad M_{\mu\mu} + M_{\tau\tau} \sim 2\sigma M_{\mu\tau}, \tag{45}$$
are satisfied, and
- For IMH, either $M_{e\mu}$, $M_{e\tau}$, $M_{\mu\mu}$ and $M_{\tau\tau}$ can vanish and
$$|M_{ee}| \sim |M_{\mu\mu} + M_{\tau\tau}| \gg |\sigma M_{e\mu} + M_{e\tau}|, \quad M_{\mu\mu} + M_{\tau\tau} \sim -2\sigma M_{\mu\tau}, \tag{46}$$
are satisfied,

where σ reflects the sign of $\sin\vartheta_{23}$. As a result, the constraint of C1) works in the textures for NMH and IMH with $m_1 \sim m_2$ while the constraint of C2) works in the textures for IMH with $m_1 \sim -m_2$. It can be generally expected that these relations are satisfied in any other models.

The effective neutrino mass of $m_{\beta\beta}$ is found to be bounded as $|m_{\beta\beta}| \lesssim 0.008$ eV for NMH and $|m_{\beta\beta}| \lesssim 0.07$ eV for IMH. This predicted maximal value of $m_{\beta\beta}$ is outside of 0.22 eV$\lesssim|m_{\beta\beta}|\lesssim$1.6 eV [30] obtained from the Heidelberg-Moscow experiment [33]. Therefore, none of the textures examined in this article is compatible with this observation if it is confirmed by other experiments. Which are appropriate textures if future experiments [28] point to, say, $\sin\theta_{13}$ =0.01, 0.1 or 0.2? The results are shown in TABLE VII, which can be readily read off from the figures. At first glance, the textures suggested by the μ-τ symmetry have any values of $\sin\vartheta_{13}$. It is because the μ-τ symmetry may represent an underlying symmetry of neutrino oscillations if it exists at all. On the other hand, the textures with one vanishing matrix element need to be strongly constrained to explain the observed data. The larger values of $\sin\vartheta_{13}$ are favored unless the appropriate nonvanishing elements are extremely suppressed.

APPENDIX A: NEUTRINO MASSES AND MIXING ANGLES

After a simple diagonalization of M by U, one can find the following conditions:

$$c_{12}\Delta_1 - s_{12}c_{13}\left(s_{13}X + \Delta_2\right) = 0, \quad s_{12}\Delta_1 + c_{12}c_{13}\left(s_{13}X + \Delta_2\right) = 0, \tag{A1}$$
$$s_{12}\left[c_{12}\lambda_1 - s_{12}\left(c^2_{13}X - s_{13}\Delta_2\right)\right] + c_{12}\left[c_{12}\left(c^2_{13}X - s_{13}\Delta_2\right) - s_{12}\lambda_2\right] = 0 \tag{A2}$$

with

$$\begin{aligned}\Delta_1 &= c_{13}s_{13}\left(M_{ee} - \lambda_3\right) + \left(c^2_{13} - s^2_{13}\right)\left(s_{23}M_{e\mu} + c_{23}M_{e\tau}\right),\\ \Delta_2 &= \left(c^2_{23} - s^2_{23}\right)M_{\mu\tau} + s_{23}c_{23}\left(M_{\mu\mu} - M_{\tau\tau}\right),\end{aligned} \tag{A3}$$

where

$$\begin{aligned}&\lambda_1 = c^2_{13}M_{ee} + s^2_{13}\lambda_3 - 2s_{13}c_{13}Y, \quad \lambda_2 = c^2_{23}M_{\mu\mu} + s^2_{23}M_{\tau\tau} - 2s_{23}c_{23}M_{\mu\tau},\\ &\lambda_3 = s^2_{23}M_{\mu\mu} + c^2_{23}M_{\tau\tau} + 2s_{23}c_{23}M_{\mu\tau},\end{aligned} \tag{A4}$$
$$X = \frac{c_{23}M_{e\mu} - s_{23}M_{e\tau}}{c_{13}}, \quad Y = s_{23}M_{e\mu} + c_{23}M_{e\tau}. \tag{A5}$$

The mixing angles of ϑ_{12} and ϑ_{13} are then expressed as:

$$\tan 2\vartheta_{12} = \frac{2X}{\lambda_2 - \lambda_1}, \quad \tan 2\vartheta_{13} = \frac{2Y}{\lambda_3 - M_{ee}}, \tag{A6}$$

together with

$$M_{\tau\tau} = M_{\mu\mu} + 2\frac{\cos 2\vartheta_{23}M_{\mu\tau} + s_{13}X}{\sin 2\vartheta_{23}}. \tag{A7}$$

The neutrino masses of $m_{1,2,3}$ are given by[5]

$$\begin{aligned} m_1 &= c_{12}^2\lambda_1 + s_{12}^2\lambda_2 - 2s_{12}c_{12}X, \quad m_2 = s_{12}^2\lambda_1 + c_{12}^2\lambda_2 + 2s_{12}c_{12}X, \\ m_3 &= s_{13}^2 M_{ee} + c_{13}^2\lambda_3 + 2s_{13}c_{13}Y, \end{aligned} \tag{A8}$$

and $m_{1,2}$ can be converted into

$$m_1 = \frac{\lambda_1+\lambda_2}{2} - \frac{X}{\sin 2\vartheta_{12}}, \quad m_2 = \frac{\lambda_1+\lambda_2}{2} + \frac{X}{\sin 2\vartheta_{12}}, \tag{A9}$$

by using Eq.(A6). These expressions are further simplified into

$$m_1 = \frac{c_{12}^2\lambda_1 - s_{12}^2\lambda_2}{c_{12}^2 - s_{12}^2}, \quad m_2 = \frac{c_{12}^2\lambda_2 - s_{12}^2\lambda_1}{c_{12}^2 - s_{12}^2}. \tag{A10}$$

These relations of masses and mixings enable us to discuss constraints on flavor neutrino masses.

[1] Y. Fukuda *et al.*. [Super-Kamiokande Collaboration], Phys. Rev. Lett. **81**, 1158 (1998); [Erratum-ibid **81**, 4279 (1998)]; Phys. Rev. Lett. **82**, 2430 (1999). See also, T. Kajita and Y. Totsuka, Rev. Mod. Phys. **73**, 85 (2001).

[2] J.N. Bahcall, W.A. Fowler, I. Iben and R.L. Sears, Astrophysics J. **137**, 344 (1963); J. Bahcall, Phys. Rev. Lett. **12**, 300 (1964); R. Davis, Jr., Phys. Rev. Lett. **12**, 303 (1964); R. Davis, Jr., D.S. Harmer and K.C. Hoffman, Phys. Rev. Lett. **20**, 1205 (1968); J.N. Bahcall, N.A. Bahcall and G. Shaviv, Phys. Rev. Lett. **20**, 1209 (1968); J.N. Bahcall and R. Davis, Jr., Science **191**, 264 (1976).

[3] Q.A. Ahmed. *et al.*, [SNO Collaboration], Phys. Rev. Lett. **87**, 071301 (2001); Phys. Rev. Lett. **89**, 011301 (2002); S. H. Ahn, *et al.*, [K2K Collaboration], Phys. Lett. B **511**, 178 (2001); Phys. Rev. Lett. **90**, 041801 (2003); K. Eguchi, *et al.*, [KamLAND collaboration], Phys. Rev. Lett. **90**, 021802 (2003); M. Apollonio, *et al.*, [CHOOZ Collaboration], Euro. Phys. J. C **27**, 331 (2003).

[4] B. Pontecorvo, Sov. Phys. JETP **34**, 247 (1958); Zh. Eksp. Teor. Piz. **53**, 1717 (1967); Z. Maki, M. Nakagawa and S. Sakata, Prog. Theor. Phys. **28**, 870 (1962).

[5] T. Yanagida, in *Proceedings of the Workshop on Unified Theories and Baryon Number in the Universe* edited by A. Sawada and A. Sugamoto (KEK Report No.79-18, Tsukuba, 1979), p.95; Prog. Theor. Phys. **64**, 1103 (1980); M. Gell-Mann, P. Ramond and R. Slansky, in *Supergravity* edited by P. van Nieuwenhuizen and D.Z. Freedmann (North-Holland, Amsterdam 1979), p.315; R.N. Mohapatra and G. Senjanović, Phys. Rev. Lett. **44**, 912 (1980). See also, P. Minkowski, Phys. Lett. **B67**, 421 (1977).

[6] R.N. Mohapatra and G. Senjanović, Phys. Rev. D **23**, 165 (1981); C. Wetterich, Nucl. Phys. B **187**, 343 (1981). See also, J. Schechter and J.W.F. Valle, Phys. Rev. D **22**, 2227 (1980).

[7] A. Zee, Phys. Lett. **93B**, 389 (1980); Phys. Lett. **161B**, 141 (1985); L. Wolfenstein, Nucl. Phys. B **175**, 93 (1980); S. T. Petcov, Phys. Lett. **115B**, 401 (1982).

[8] A. Zee, Nucl. Phys. **264B**, 99 (1986); K. S. Babu, Phys. Lett. B **203**, 132 (1988); D. Chang, W-Y. Keung and P.B. Pal, Phys. Rev. Lett. **61**, 2420 (1988); J. Schechter and J.W.F. Valle, Phys. Lett. B **286**, 321 (1992).

[9] See for example, R.N. Mohapatra, *et al.*,"Theory of Neutrinos", [arXive:hep-ph/0412099]. See also, S. Goswami, Talk given at *Neutrino 2004: The 21st International Conference on Neutrino Physics and Astrophysics*, Paris, France (June 14-19, 2004); G. Altarelli, Talk given at *Neutrino 2004: The 21st International Conference on Neutrino Physics and Astrophysics*, Paris, France (June 14-19, 2004); A. Bandyopadhyay, Phys. Lett. B **608**, 115 (2005).

[10] O. Mena and S. Parke, Phys. Rev. D **69**, 117301 (2004);

[11] T. Fukuyama and H. Nishiura, in *Proceedings of International Workshop on Masses and Mixings of Quarks and Leptons* edited by Y. Koide (World Scientific, Singapore, 1997), p.252; "Mass Matrix of Majorana Neutrinos", [arXive:hep-ph/9702253]; Y. Koide, H. Nishiura, K. Matsuda, T. Kikuchi and T. Fukuyama, Phys. Rev. D **66**, 093006 (2002); Y. Koide, Phys. Rev. D **69**, 093001 (2004); K. Matsuda and H. Nishiura, Phys. Rev. D **69**, 117302 (2004).

[12] See for example, C.S. Lam, Phys. Lett. B **507**, 214 (2001); W. Grimus and L. Lavoura, JHEP **0107**, 045 (2001); Euro. Phys. J. C **28**, 123 (2003); Phys. Lett. B **572**, 189 (2003); J. Phys. G **30**, 73 (2004); T. Kitabayashi and M. Yasuè, Phys. Lett. B **524**, 308 (2002); Int. J. Mod. Phys. A **17**, 2519 (2002); Phys. Rev. D **67**, 015006 (2003); P.F. Harrison and W.G. Scott, Phys. Lett. B **547**, 219 (2002); I. Aizawa, M. Ishiguro, T. Kitabayashi and M. Yasuè, Phys. Rev. D **70**, 015011 (2004); W. Grimus, A.S. Joshipura, S. Kaneko, L. Lavoura, H. Sawanaka and M. Tanimoto, JHEP **0407**, 078 (2004); "Non-Vanishing U_{e3} and $\cos 2\theta_{23}$ from a Broken Z_2 Symmetry", [arXive:hep-ph/0408123];

---

[5] In Ref.[32], Eqs.(4) and (6) should read the corresponding expressions in Eqs.(A4)-(A8) of this article.

[13] R.N. Mohapatra, JHEP **0410**, 027 (2004); R.N. Mohapatra and S. Nasri, "Leptogenesis and $\mu - \tau$ symmetry" (to appear in Phys, Rev D), [arXive:hep-ph/0410369]; R.N. Mohapatra, S. Nasri and H. Yu, "Leptogenesis, μ-τ Symmetry and ϑ_{13}", [arXive:hep-ph/0502026].

[14] See for example, F. Vissani, "A Study of the Scenario with Nearly Degenerate Majorana Neutrinos", [arXiv:hep-ph/9708483]; D. V. Ahluwalia, Mod. Phys. Lett. A **13**, 2249 (1998); V. Barger, P. Pakvasa, T.J. Weiler and K. Whisnant, Phys. Lett. B **437**, 107 (1998); A.J. Baltz, A.S. Goldhaber and M. Goldhaber, Phys. Rev. Lett. **81**, 5730 (1998); M. Jezabek and Y. Sumino, Phys. Lett. B **440**, 327 (1998); R.N. Mohapatra and S. Nussinov, Phys. Lett. B **441**, 299 (1998);, Phys. Rev. D **60**, 013002 (1999); Y. Nomura and T. Yanagida, Phys. Rev. D **59**, 017303 (1999); I. Starcu and D.V.Ahluwalia, Phys. Lett. B **460**, 431 (1999); Q. Shafi and Z. Tavartkiladze, Phys. Lett. B **451**, 129 (1999); Phys. Lett. B **482**, 145 (2000); C.H. Albright and S.M. Barr, Phys. Lett. B **461**, 218 (1999); H. Georgi and S.L. Glashow, Phys. Rev. D **61**, 097301 (2000); R.N. Mohapatra, A. Pérez-Lorenzana and C. A. de S. Pires, Phys. Lett. B **474**, 355 (2000); T. Kitabayashi and M. Yasuè, Phys. Lett. B **490**, 236 (2000); Phys. Rev. D **63**, 095002 (2001); Phys. Rev. D **63**, 095006 (2001); Phys. Lett. B **508**, 85 (2001); Nucl. Phys. B **609**, 61 (2001); B. Brahmacari and S. Choubey, Phys. Lett. B **531**, 99 (2002); K. S. Babu and R. N. Mohapatra, Phys. Lett. B **532**, 77 (2002); T. Ohlsson and G. Seidl, Phys. Lett. B **537**, 95 (2002); R. Kuchimanchi and R. N. Mohapatra, Phys. Rev. D **66**, 051301(R) (2002); C. Giunti and M. Tanimoto, Phys. Rev. D **66**, 053013 (2002).

[15] R. Barbieri, L.J. Hall, D. Smith, N.J. Weiner and A. Strumia, JHEP **12**, 017 (1998). See also S.T. Petcov, Phys. Lett. **110B**, 245 (1982); C.N. Leung and S.T. Petcov, Phys. Lett. **125B**, 461 (1983); A. Zee, Phys. Lett. **161B**, 141 (1985).

[16] See for example, P.F. Harrison, D.H. Perkins and W.G. Scott, Phys. Lett. B **349**, 137 (1995); Phys. Lett. B **530**, 167 (2002); Z.-Z. Xing, Phys. Lett. B **533**, 85 (2002); P.F. Harrison and W.G. Scott, Phys. Lett. B **535**, 163 (2002); Phys. Lett. B **557**, 76 (2003); Phys. Lett. B **594**, 324 (2004); C.I. Low and R.R. Volkas, Phys. Rev. D **68**, 033007 (2003); X.-G. He and A. Zee, Phys. Lett. B **560**, 87 (2003); N. Li and Bo-Q. Ma, Phys. Rev. D **71**, 017302 (2005).

[17] P.F. Harrison and W.G. Scott, Int. J. Mod. Phys. A **18**, 3957 (2003).

[18] H. Fritzsch and Z.Z. Xing, Phys. Lett. B **372**, 265 (1996); Phys. Lett. B **440**, 313 (1998); M. Fukugita, M. Tanimoto and T. Yanagida, Phys. Rev. D **57**, 4429 (1998); M. Tanimoto, Phys. Rev. D **59**, 017304 (1999).

[19] M. Apollonio *et al.* [CHOOZ Collaboration], Euro. Phys. J. C **27**, 331 (2003); E. Kearns *et al.* [Super-Kamiokande Collaboration], Talk given at *Neutrino 2004: The 21st International Conference on Neutrino Physics and Astrophysics*, Paris, France (June 14-19, 2004); T. Nakaya *et al.* [K2K Collaboration], Talk given at *Neutrino 2004: The 21st International Conference on Neutrino Physics and Astrophysics*, Paris, France (June 14-19, 2004); T. Araki *et al.* [KamLAND Collaboration], "Measurement of Neutrino Oscillation with KamLAND: Evidence of Spectral Distortion", [arXive:hep-ex/0406035].

[20] H. Nishiura, K. Matsuda and T. Fukuyama, Phys. Rev. D60, 013006 (1999); M.-C. Chen and K.T. Mahanthappa, Phys. Rev. D **62**, 113007 (2000); S.K. Kang and C.S. Kim, Phys. Rev. D **63**, 113010 (2001).

[21] See for example, P.H. Frampton, S.L. Glashow and D. Marfatia, Phys. Lett. B **536**, 79 (2002); Z. Z. Xing, Phys. Lett. B **530**, 159 (2002), Phys. Lett. B **539**, 85 (2002), Phys. Rev. D **69**, 013006 (2004); P. H. Frampton, S. L. Glashow and T. Yanagida, Phys. Lett. B **548**, 119 (2002); A. Kageyama, S. Kaneko, N. Shimoyama and M. Tanimoto, Phys. Lett. B **538**, 96 (2002); M. Raidal and A. Strumia, Phys. Lett. B **553**, 72 (2003); R. Barbieri, T. Hambye and A. Romanino, JHEP **0303**, 017 (2003); B.R. Desai, D.P. Roy and A.R. Vaucher, Mod. Phys. Lett. A **18**, 1355 (2003); M. Bando, S. Kaneko, M. Obara and M. Tanimoto, Phys. Lett. B **580**, 229 (2004); L. Lavoura, Phys. Lett. B **609**, 317 (2005); W. Grimus and L. Lavoura, "On a Model with Two Zeros in the Neutrino Mass Matrix", [arXive:hep-ph/0412283].

[22] G. C. Branco, R. G. Felipe, F. R. Joaquim and T. Yanagida, Phys. Lett. B **562**, 265 (2003).

[23] D. Black, A. H. Fariborz, S. Nasri and J. Schechter Phys. Rev. D **62**, 073015 (2000); X.-G. He and A. Zee, Phys. Rev. D **68**, 037302 (2003); W. Rodejohann, Phys. Lett. B **579**, 127 (2004).

[24] T. Asaka, M. Fujii, K. Hamaguchi and T. Yanagida, Phys. Rev. D **62**, 123514 (2000); M. Fujii, K. Hamaguchi and T. Yanagida, Phys. Rev. D **64**, 123526 (2001).

[25] I. Affleck and M. Dine, Nucl. Phys. B **249**, 361 (1985).

[26] M. Fukugida and T. Yanagida, Phys. Lett. B **174**, 45 (1986).

[27] See for example, H. Minakata, H. Sugiyama and O. Yasuda, K. Inoue and F. Suekane, Phys. Rev. D **68**, 033017 (2003); C. Lunardini and A.Yu. Smirnov, JCAP **06**, 009 (2003); J. Bernabeu, S.P. Ruiz and S.T. Petcov, Nucl. Phys. B **669**, 255 (2003); O. Yasuda, "Measurement of $\sin^2 2\theta_{13}$ by reactor experiments and its sensitivity", Talk presented at Coral Gables Conference On Lauching Of Belle Epoque In High-Energy Physics And Cosmology (CG 2003), 17-21 Dec 2003, Ft. Lauderdale, Florida, [arXive:hep-ph/0403162]; Q. Shafi and Z. Tavartkiladze, Phys. Lett. B **594**, 177 (2004); O.L.G. Peres and A.Yu. Smirnov, Nucl. Phys. B **680**, 479 (2004); A. Romanino, Phys. Rev. D **70**, 013003 (2004); J.W. Mei and Z.Z. Xing, Phys. Rev. D **70**, 053002 (2004); S. P. Ruiz and S.T. Petcov, Nucl. Phys. B **712**, 392 (2005); N.N. Singh and M.K. Das, "Radiative Generation of Δm^2_{21} and in Two-fold Degenerate Neutrino Models", [arXive:hep-ph/0407206]; J. Ferrandis and S. Pakvasa, Phys. Lett. B **603**, 184 (2004); S. Goswami and A.Yu. Smirnov. "Solar Neutrinos and 1-3 Leptonic Mixing", [arXive:hep-ph/0411359].

[28] See for example, A. Guglielmi, Phys. At. Nucl. **67**, 1129 (2004); M. Goodman, "Plans for Experiments to Measure θ_{13}", [arXive:hep-ex/0404031]; S. Rigolin, "Why Care about (θ_{13}, δ) Degeneracy at Future Neutrino Experiments", [arXive:hep-ph/0407009]; Th. Lasserre, "Chasing Theta(13) with New Reaxtor Neutrino Experiments", [arXive:hep-ex/0411083]; A.Ferrari. A. Guglielmi and P.R, Sala, "CNGS Neutrino Beam Systematics for θ_{13}, [arXive: hep-ph/0501283].

[29] I. Aizawa and M. Yasuè, Phys. Lett. B **607**, 267 (2005).

[30] See for example, C. Giunti, "Phenomenology of Absolute Neutrino Masses", talk given at *NOW-2004, Neutrino Oscillation Workshop*, Conca Specchiulla, Otranto, Italy (Sep. 11-17, 2004), [arXive: hep-ph/0412148] and references therein.

[31] See for example, M. Frigerio and A.Yu. Smirnov, Nucl. Phys. B **640**, 233 (2002).
[32] I. Aizawa, M. Ishiguro, T. Kitabayashi and M. Yasuè, in Ref.[12].
[33] H.V. Klapdor-Kleingrothaus *et al.*, Euro. Phys. J. A **12**, 147 (2001).

TABLE I: General constraints on flavor neutrino masses of M_{ij} for $i, j = e, \mu, \tau$ that provide $\sin^2 2\vartheta_{atm} \sim 1$, $\sin^2\vartheta_{13} \ll 1$, $\sin^2 2\vartheta_\odot \gg \sin^2\vartheta_{13}$, and $\Delta m^2_{atm} \gg \Delta m^2_\odot$, where $\cos\vartheta_{23} \sim \sigma\sin\vartheta_{23} \sim 1/\sqrt{2}$ ($\sigma = \pm 1$). In $\Delta m^2_{atm} \gg \Delta m^2_\odot$, $|M_{\mu\mu} + M_{\tau\tau}| \gg |M_{ee}|$ is satisfied if $M_{\mu\mu} + M_{\tau\tau} \sim 2\sigma M_{\mu\tau} + 2M_{ee}$ is chosen for $\sin^2 2\vartheta_\odot \gg \sin^2\vartheta_{13}$.

<table>
<tr><th colspan="2">assumption</th><th colspan="2">$\sin^2 2\vartheta_{atm} \sim 1$</th><th>$\sin^2\vartheta_{13} \ll 1$</th><th>$\sin^2 2\vartheta_\odot \gg \sin^2\vartheta_{13}$</th><th>$\Delta m^2_{atm} \gg \Delta m^2_\odot$</th></tr>
<tr><td colspan="2">NMH</td><td colspan="3">$M_{e\tau} \sim -\sigma M_{e\mu}$
and/or</td><td>$M_{\mu\mu} + M_{\tau\tau} \sim 2\sigma M_{\mu\tau} + 2M_{ee}$
and/or
$|M_{e\mu} - \sigma M_{e\tau}| \gg |\sigma M_{e\mu} + M_{\mu\tau}|$</td><td>$M_{\mu\mu} + M_{\tau\tau} \sim 2\sigma M_{\mu\tau}$
$(*)|M_{\mu\mu} + M_{\tau\tau}| \gg |M_{ee}|$</td></tr>
<tr><td rowspan="2">IMH</td><td>$m_1 \sim m_2$</td><td rowspan="2">$M_{e\tau} \sim \sigma M_{e\mu}$
and
$M_{\mu\mu} \sim M_{\tau\tau}$</td><td rowspan="2">$M_{\mu\mu} \sim M_{\tau\tau}$</td><td rowspan="2">$|M_{ee,\mu\mu,\mu\tau \text{ and/or } \tau\tau}|$
$\gg |\sigma M_{e\mu} + M_{\mu\tau}|$</td><td>$M_{\mu\mu} + M_{\tau\tau} \sim 2\sigma M_{\mu\tau} + 2M_{ee}$</td><td rowspan="2">$M_{\mu\mu} + M_{\tau\tau} \sim -2\sigma M_{\mu\tau}$
$M_{\mu\mu} + M_{\tau\tau} \sim 2\sigma M_{\mu\tau} \pm 2M_{ee}$
$(*)\pm$ for $m_1 \sim \pm m_2$</td></tr>
<tr><td>$m_1 \sim -m_2$</td><td>$|M_{e\mu} - \sigma M_{e\tau}| \gg |\sigma M_{e\mu} + M_{\mu\tau}|$</td></tr>
</table>

TABLE II: The upper and lower limits of m_3^2/m_2^2 with the normal mass hierarchy (NMH) and of m_2^2/m_1^2 with inverted mass hierarch (IMH) in models based on $\det(M) = 0$ with specific textures, where the mass ratios are calculated from Eqs.(25) and (26) with the observed mixing angles in Eq.(1). The values in the parentheses are those for $\sin\theta_{23} < 0$.

assumption	m_3^2/m_2^2 (NMI)		m_2^2/m_1^2 (IMH)	
bound	lower	upper	lower	upper
$M_{ee} = 0$	16.5(16.5)	$\infty(\infty)$	2.49(2.49)	11.6(11.6)
$M_{e\mu} = 0$	2.55(4.21)	$\infty(\infty)$	1.00(0.26)	2.64(1.00)
$M_{e\tau} = 0$	2.53(1.29)	$\infty(\infty)$	0.14(1.00)	1.00(3.54)
$M_{\mu\mu} = 0$	0.19(0.82)	1.91(3.03)	0.09(0.09)	2.48(0.40)
$M_{\mu\tau} = 0$	0.38(0.38)	0.74(0.65)	0.09(0.06)	0.40(0.64)
$M_{\tau\tau} = 0$	0.12(0.04)	1.06(0.59)	0.09(0.09)	0.04(4.56)
$M_{\mu\mu} = M_{\tau\tau}$	$\sim 0(0.36)$	$1.39 \times 10^4(1.42 \times 10^4)$	$0.09(\sim 0)$	$\sim\infty(0.37)$
$M_{e\tau} = M_{e\mu}$	166(0.42)	$\infty(\infty)$	$0.85(\sim 0)$	1.00(11.4)
$M_{e\tau} = -M_{e\mu}$	$\sim 0(154)$	$\infty(\infty)$	1.00(1.00)	$\sim\infty(1.17)$

TABLE III: The predictions of $\sin\vartheta_{13}$ depending on the sign of $\sin\vartheta_{23}$ given by ± for NMH and IMH, where the excluded cases are denoted by the dots. The absence of the allowed M_{ee} for IMH is due to Eq.(23)

assumption	NMI		IMH	
$\sin\vartheta_{23}$	+	−	+	-
$M_{ee} = 0$	$0.153 \sim$		$\cdots$	$\cdots$
$M_{e\mu} = 0$	$0.043 \sim 0.159$	$0.045 \sim 0.197$	$0.001 \sim 0.023$	$\cdots$
$M_{e\tau} = 0$	$0.034 \sim 0.147$	$0.032 \sim 0.119$	$\cdots$	$0.001 \sim 0.017$
$M_{\mu\mu} = 0$	$\cdots$	$\cdots$	$0.115 \sim$	$\cdots$
$M_{\mu\tau} = 0$	$\cdots$	$\cdots$	$\cdots$	$\cdots$
$M_{\tau\tau} = 0$	$\cdots$	$\cdots$	$\cdots$	$0.086 \sim$
$M_{\mu\mu} = M_{\tau\tau}$	$0.006 \sim$	$0.009 \sim$	$0.0002 \sim$	$\cdots$
$M_{e\tau} = M_{e\mu}$	$\cdots$	$0.008 \sim 0.021$	$\cdots$	$0.001 \sim$
$M_{e\tau} = -M_{e\mu}$	$0.007 \sim 0.017$	$\cdots$	~ 0.003	$0.009 \sim$

TABLE IV: The same as in TABLE III but for $|m_{\beta\beta}|$ in the unit of eV.

assumption	NMI		IMH	
$\sin\vartheta_{23}$	$+$	$-$	$+$	-
$M_{ee}=0$	0	0	0	0
$M_{e\mu}=0$	$0.001\sim0.004$	$0.002\sim0.005$	$0.03\sim0.07$	$\cdots$
$M_{e\tau}=0$	$0.002\sim0.004$	$0.001\sim0.004$	$\cdots$	$0.03\sim0.07$
$M_{\mu\mu}=0$	$\cdots$	$\cdots$	$0.008\sim0.03$	$\cdots$
$M_{\mu\tau}=0$	$\cdots$	$\cdots$	$\cdots$	$\cdots$
$M_{\tau\tau}=0$	$\cdots$	$\cdots$	$\cdots$	$0.007\sim0.04$
$M_{\mu\mu}=M_{\tau\tau}$	$0.00001\sim0.004$	$0.002\sim0.008$	$0.007\sim0.07$	$\cdots$
$M_{e\tau}=M_{e\mu}$	$\cdots$	$0.002\sim0.004$	$\cdots$	$0.007\sim0.04$
$M_{e\tau}=-M_{e\mu}$	$0.002\sim0.004$	$\cdots$	$0.03\sim0.07$	$0.03\sim0.07$

TABLE V: The list of calculated values of the flavor neutrino masses in the unit of m_2 in the allowed textures for NMH with the specific mixing angles of $\sin 2\vartheta_{12}=0.80$, $\sin 2\vartheta_{23}=0.98$ (or $\sin 2\vartheta_{23}=0.998$) and the typical values of $\sin\vartheta_{13}$, where σ ($=\pm1$) stands for the sign of $\sin\vartheta_{23}$.

condition	$\sin^2\vartheta_{12}$	$\sin^2\vartheta_{23}$	$\sin\vartheta_{13}$	σ	M_{ee}	$M_{e\mu}$	$M_{e\tau}$	$M_{\mu\mu}+M_{\tau\tau}$	$2\sigma M_{\mu\tau}$
$M_{ee}=0$	0.80	0.98	0.20	$+$	0	-0.56	-1.31	-5.63	-7.04
				$-$	0	1.21	-0.74	-5.63	-6.98
$M_{e\mu}=0$	0.80	0.98	0.10	$+$	0.225	0	-0.68	-4.11	-5.51
				$-$	0.328	0	0.68	6.11	4.62
$M_{e\tau}=0$	0.80	0.98	0.09	$+$	0.31	0.59	0	5.28	3.78
				$-$	0.24	0.59	0	-3.28	-4.66
$M_{\mu\mu}=M_{\tau\tau}$	0.80	0.998	0.22	$+$	0.076	-0.30	-0.95	-2.95	-4.40
				$-$	0.52	-0.44	-1.09	5.84	4.40
$M_{e\tau}=M_{e\mu}$	0.80	0.98	0.05	$+$	$\cdots$	$\cdots$	$\cdots$	$\cdots$	$\cdots$
				$-$	0.28	0.32	0.32	7.36	5.85
$M_{e\tau}=-M_{e\mu}$	0.80	0.98	0.05	$+$	0.28	0.32	-0.32	-5.36	-6.74
				$-$	$\cdots$	$\cdots$	$\cdots$	$\cdots$	$\cdots$

TABLE VI: The same as in TABLE.V but in the unit of m_1 for the allowed textures for IMH, where $\lambda_{1,2}$ are included to see $m_1\sim\pm m_2$ for $\lambda_1\sim\pm\lambda_2$ and $\sin^2 2\theta_{12}=0.90$ is chosen in the texture with $M_{\mu\mu}=0$ instead of $\sin^2 2\theta_{12}=0.80$.

condition	$\sin^2\vartheta_{12}$	$\sin^2\vartheta_{23}$	$\sin\vartheta_{13}$	σ	λ_1	λ_2	M_{ee}	$M_{e\mu}$	$M_{e\tau}$	$M_{\mu\mu}+M_{\tau\tau}$	$2\sigma M_{\mu\tau}$
$M_{e\mu}=0$	0.80	0.98	0.100	$+$	1.01	1.01	1.01	0	-0.01	1.01	-1.00
$M_{e\tau}=0$	0.80	0.98	0.100	$-$	1.01	1.02	1.01	0.02	0	1.02	-1.01
$M_{\mu\mu}=0$	0.90	0.98	0.190	$+$	0.31	-0.32	0.30	-0.75	0.57	-0.31	0.38
$M_{\tau\tau}=0$	0.80	0.98	0.210	$-$	0.44	-0.46	0.42	-0.61	-0.65	-0.45	0.43
$M_{\mu\mu}=M_{\tau\tau}$	0.80	0.98	0.037	$+$	0.44	-0.47	0.44	-0.70	0.58	-0.47	0.48
$M_{e\tau}=M_{e\mu}$	0.80	0.98	0.145	$-$	0.44	-0.46	0.43	-0.63	-0.63	-0.45	0.43
$M_{e\tau}=-M_{e\mu}$	0.80	0.98	0.001	$+$	1.01	1.02	1.01	0.01	-0.01	1.02	-1.01
	0.80	0.98	0.100	$-$	1.00	1.01	0.99	0.07	-0.07	1.02	-0.99

TABLE VII: The allowed textures denoted by ◯ for NMH and IMH that give $\sin\vartheta_{13} = 0.01, 0.1, 0.2$, where ± stand for $\sin\vartheta_{23} = \pm 1$ and the values of $A \equiv \sin^2 2\vartheta_{atm}$ and $S \equiv \sin^2 2\vartheta_{\odot}$ are shown if these angles are more constrained than those listed in Eq.(1).

$\sin\vartheta_{13}$	0.01				0.1				0.2			
assumption	NMI		IMH		NMI		IMH		NMI		IMH	
type	+	−	+	−	+	−	+	−	+	−	+	−
$M_{ee}=0$	×	×	×	×	×	×	×	×	◯	◯	×	×
$M_{e\mu}=0$	×	×	◯	×	◯	◯	×	×	×	×	×	×
$M_{e\tau}=0$	×	×	×	◯	◯	◯ $0.97 \le A$	×	×	×	×	×	×
$M_{\mu\mu}=0$	×	×	×	×	×	×	×	×	×	×	◯ $0.86 \le S$ ≤ 0.92	×
$M_{\mu\tau}=0$	×	×	×	×	×	×	×	×	×	×	×	×
$M_{\tau\tau}=0$	×	×	×	×	×	×	×	◯ $A \le 0.98$	×	×	×	◯ $0.93 \le A$ $0.75 \le S$ ≤ 0.86
$M_{\mu\mu}=M_{\tau\tau}$	◯ $A \sim 1$	◯ $A \sim 1$	◯	×	◯ $A \sim 1$	◯ $A \sim 1$	◯	×	◯ $A \sim 1$	◯ $A \sim 1$	◯	×
$M_{e\tau}=M_{e\mu}$	×	◯ $A \le 0.98$	×	◯ $0.72 \le S$ ≤ 0.92	×	×	×	◯ $0.97 \le A$	×	×	×	◯ $0.94 \le A$ ≤ 0.99
$M_{e\tau}=-M_{e\mu}$	◯ $A \le 0.97$	×	×	×	×	×	×	◯	×	×	×	◯ $0.97 \le A$

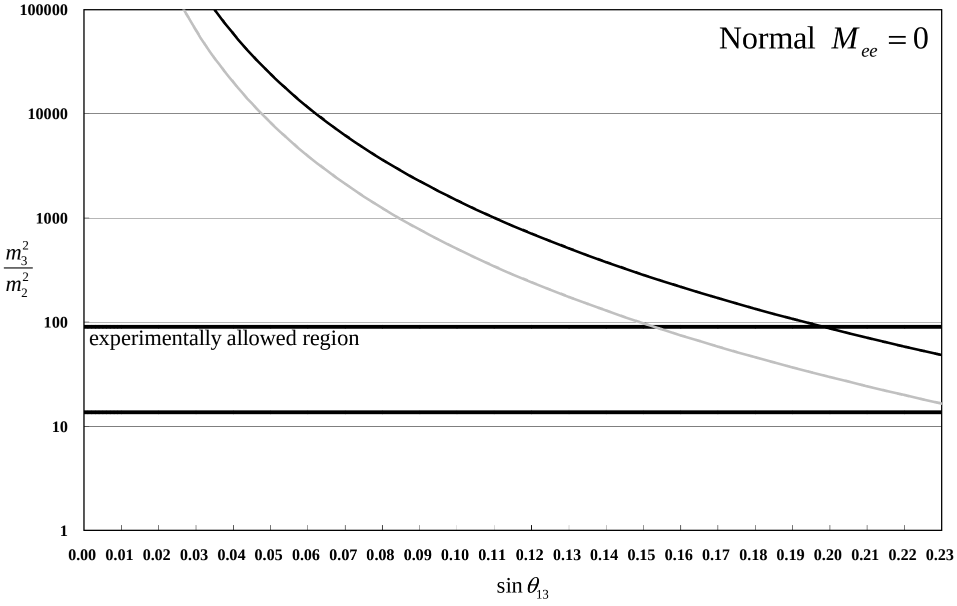

FIG. 1: The prediction of m_3^2/m_2^2 for NMH: The area between the black curve (upper bound) and the gray curve (lower bound) is our prediction on m_3^2/m_2^2 in the texture with $M_{ee} = 0$, which does not depend on the sign of $\sin\vartheta_{23}$. The area between two straight lines is the experimentally allowed region, which in turn determines the allowed values of $\sin\vartheta_{13}$.

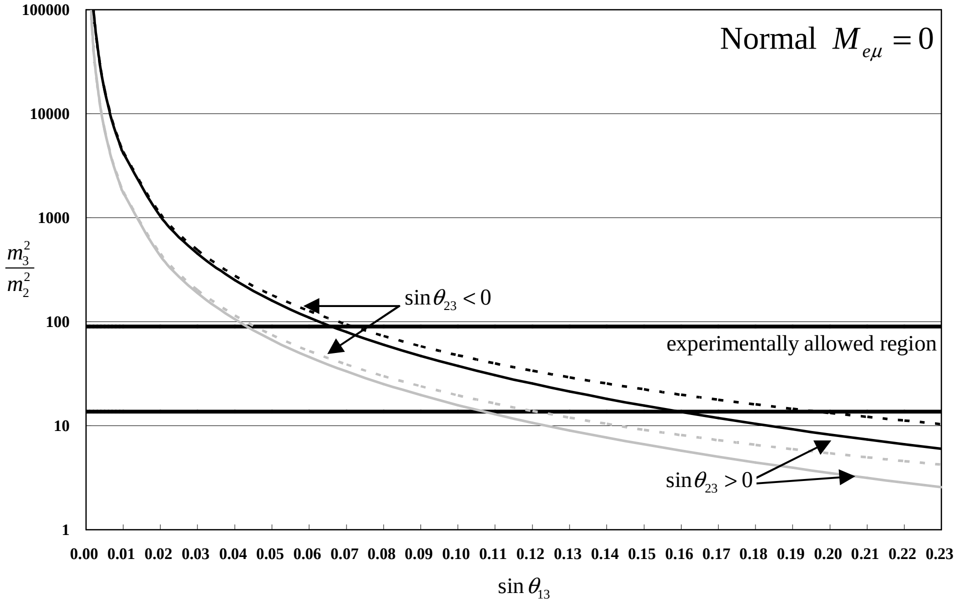

FIG. 2: The same as in FIG.1 but for $M_{e\mu}=0$. The solid (dashed) curves correspond to $\sin\theta_{23}>0$ ($\sin\theta_{23}<0$). The areas between the black curves (upper bounds) and the gray curves (lower bounds) are our predictions.

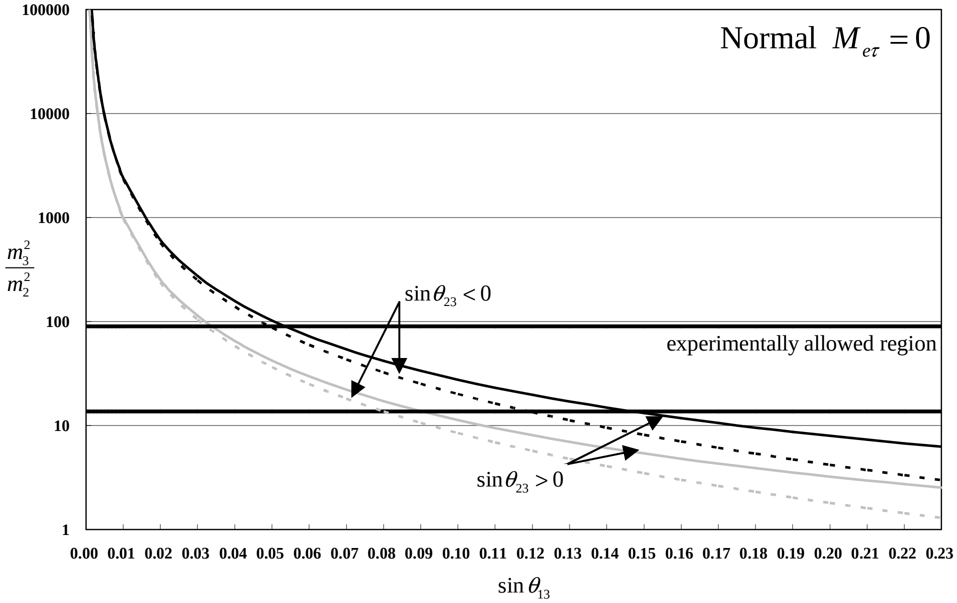

FIG. 3: The same as in FIG.2 but for $M_{e\tau}=0$.

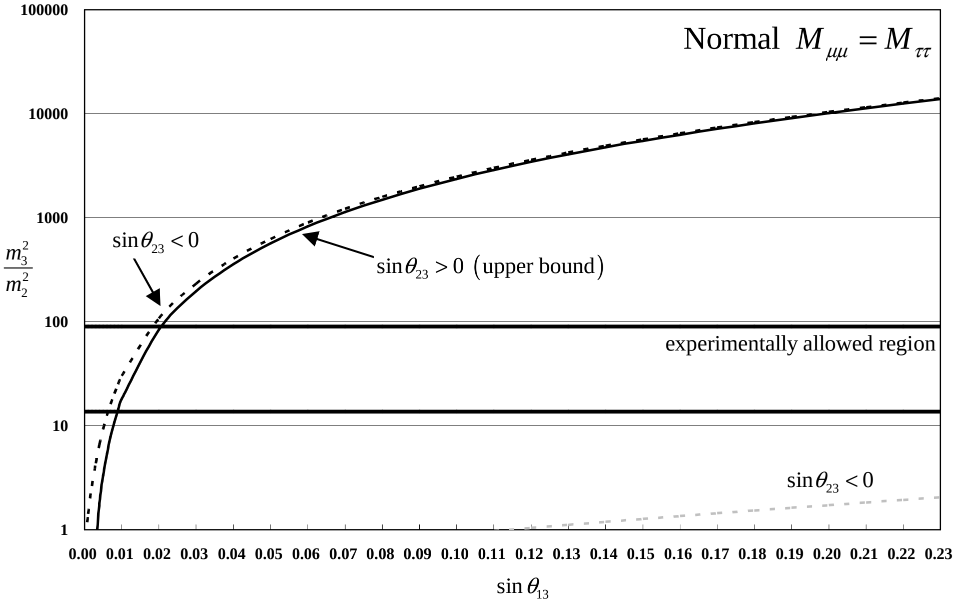

FIG. 4: The same as in FIG.2 but for $M_{\mu\mu} = M_{\tau\tau}$. The lower bound in the case of $\sin\theta_{23} > 0$ is outside the graph.

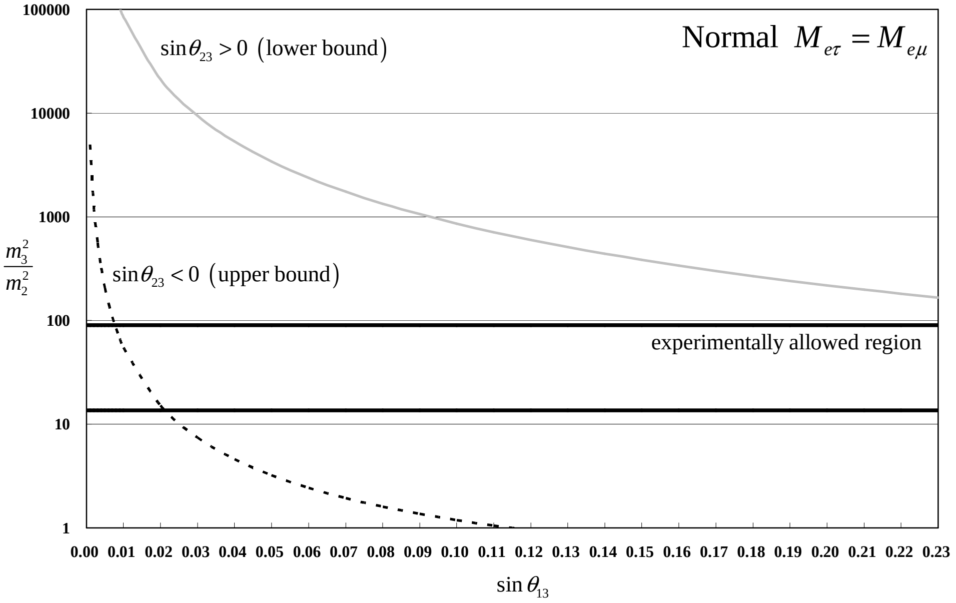

FIG. 5: The same as in FIG.2 but for $M_{e\tau} = M_{e\mu}$. The allowed region is above the grey solid curve or below the black dashed curve.

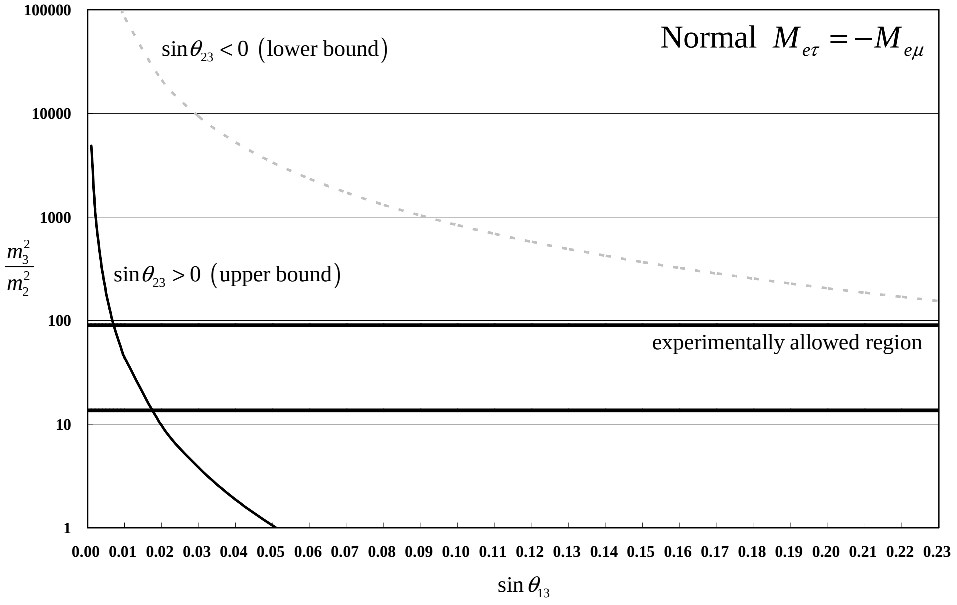

FIG. 6: The same as in FIG.2 but for $M_{e\tau} = -M_{e\mu}$. The allowed region is above the grey dashed curve or below the black solid curve.

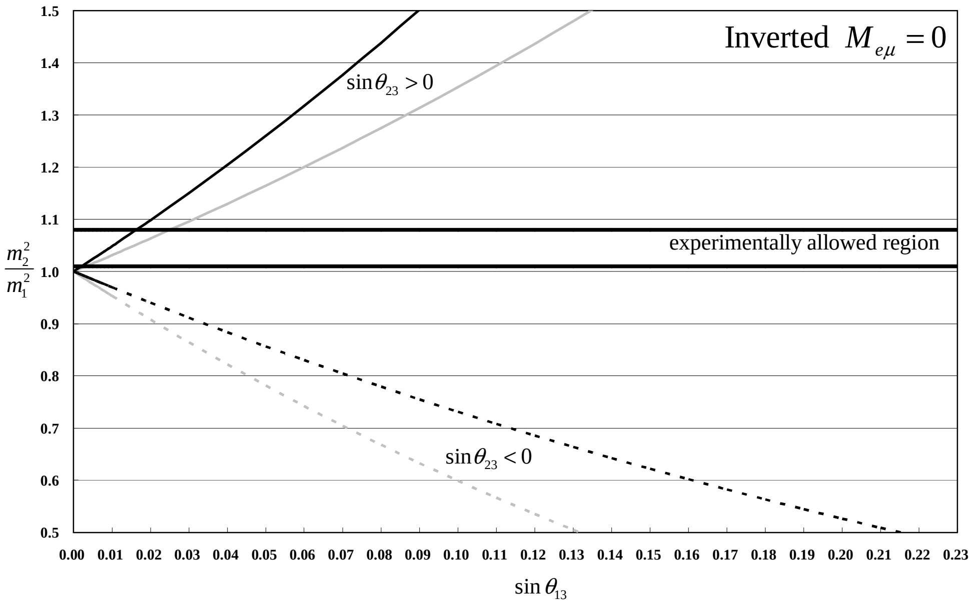

FIG. 7: The m_2^2/m_1^2 for IMH: The areas between the black curves (upper bounds) and the gray curves (lower bounds) are our predictions on m_2^2/m_1^2 in the texture with $M_{e\mu} = 0$. The solid (dashed) curves correspond to $\sin\theta_{23} > 0$ ($\sin\theta_{23} < 0$).

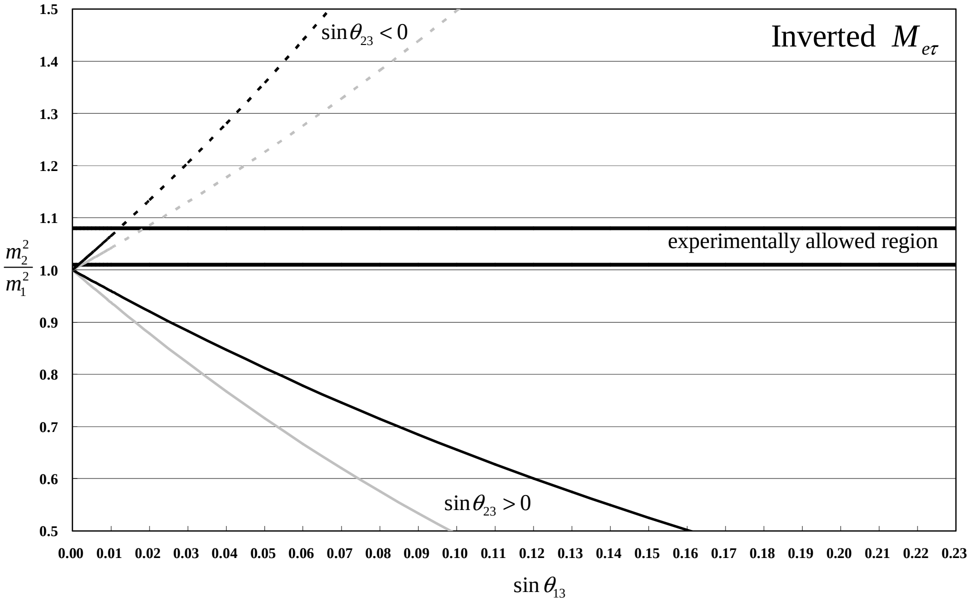

FIG. 8: The same as in FIG.7 but for $M_{e\tau} = 0$.

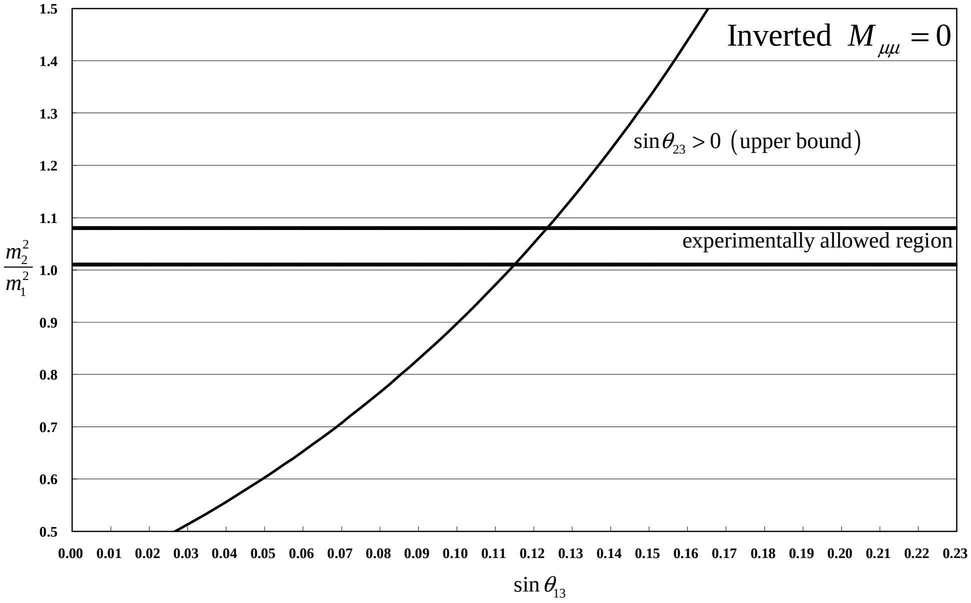

FIG. 9: The same as in FIG.7 but for $M_{\mu\mu} = 0$. The allowed region is below the black solid curve.

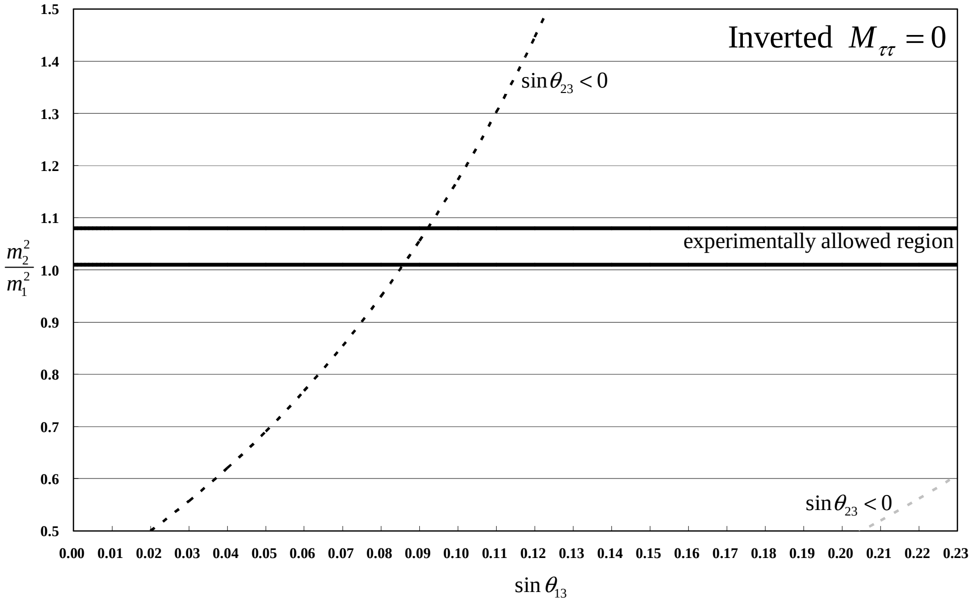

FIG. 10: The same as in FIG.7 but for $M_{\tau\tau} = 0$. The allowed region is below the black dashed curve and above the grey dashed curve.

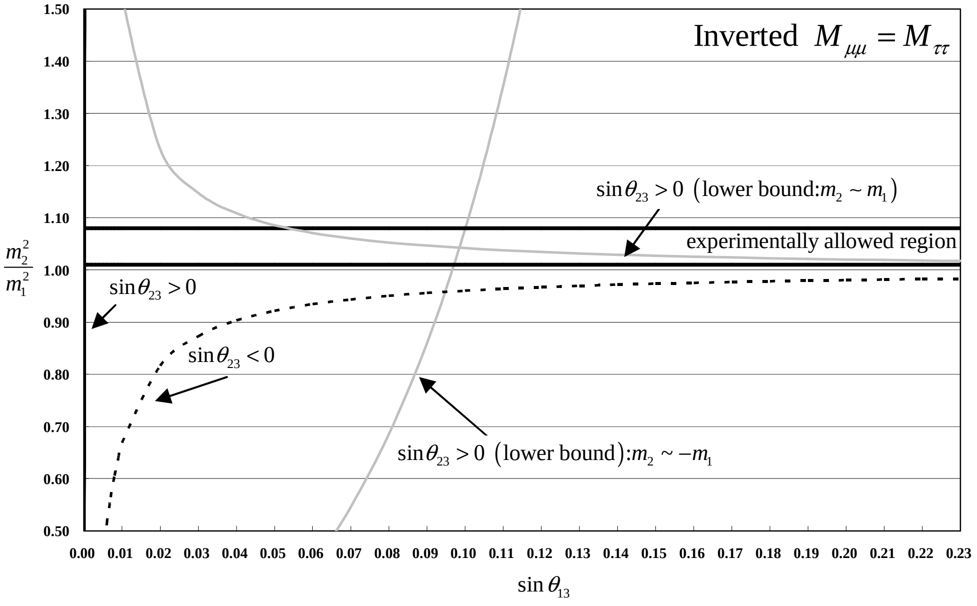

FIG. 11: The same as in FIG.7 but for $M_{\mu\mu} = M_{\tau\tau}$. Two grey solid curves represent two lower bounds for the cases with $m_2 \sim m_1$ and $m_2 \sim -m_1$. The allowed region is either above one of the grey solid curves that gives the smaller value or below the black dashed curve. For $\sin\theta_{23} > 0$, the upper bound is very steep so that it almost runs on the vertical axis.

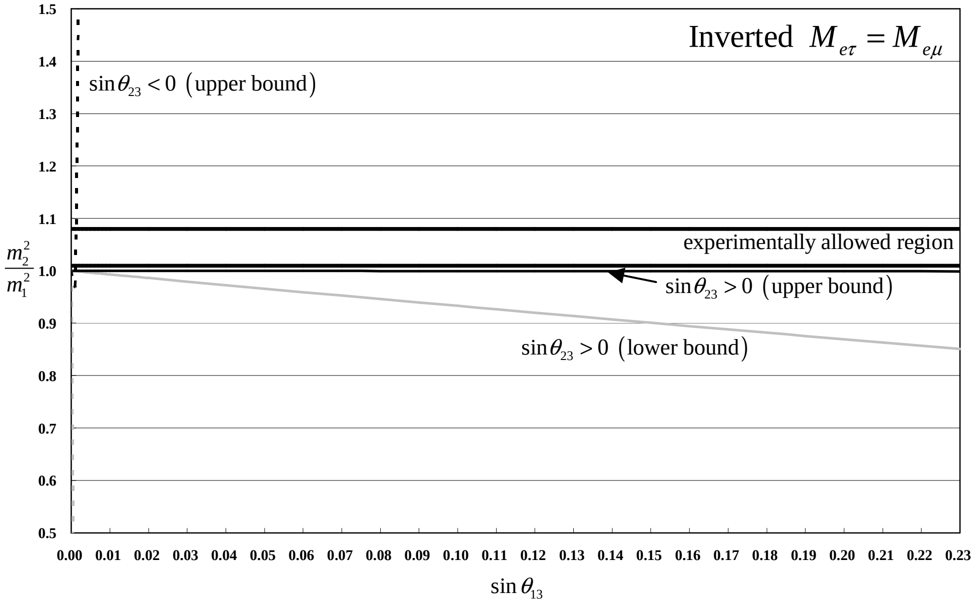

FIG. 12: The same as in FIG.7 but for $M_{e\tau} = M_{e\mu}$. The allowed regions are below the black dashed curve and the area between the black solid line at $m_2^2/m_1^2 = 1$ and the gray solid curve. The lower bound in the case of $\sin\vartheta_{23} < 0$ is outside the graph.

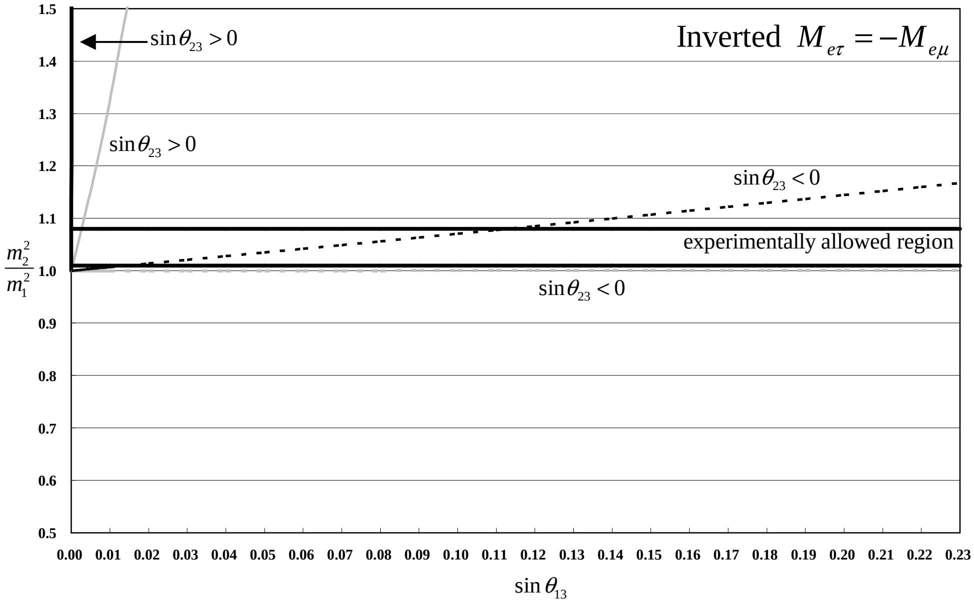

FIG. 13: The same as in FIG.7 but for $M_{e\tau} = -M_{e\mu}$. The allowed regions are the area between the black vertical line and the grey curve and the area between the black dashed curve and the gray dashed curve at $m_2^2/m_1^2 = 1$. For $\sin\theta_{23} > 0$, the upper bound in the case of $\sin\vartheta_{23} > 0$ is very steep so that it almost runs on the vertical axis.